SGG·SGS   sc | nat 🇨🇭

Swiss Journal of Geosciences

ORIGINAL PAPER

Open Access

Check for updates

Tectonics of the Western Internal Jura fold-and-thrust belt: 2D kinematic forward modelling

Adeline Marro[1]*, Louis Hauvette[1,2], Sandra Borderie[1] and Jon Mosar[1]

Abstract

The balancing technique, called 2D kinematic forward modelling, is a powerful tool to understand the kinematic evolution of fold-and-thrust belts. This study presents a new 2D kinematic forward model for the westernmost Internal Jura fold-and-thrust belt (FTB), situated immediately adjacent to the Geneva Basin. The technique used not only provides a new valid balanced cross-section but also offers new insights regarding the kinematic evolution of the Western Internal Jura FTB. Our model proposes a pure thin-skinned style dominated by forward stepping deformation accompanied by minor back-stepping thrust sequences. A first deformation step is attributed to the thrusting of the Crêt de la Neige Anticline, followed by the Crêt Chalam Thrust and its imbrications. This is followed by thrusting along the Tacon and the Bienne thrusts. Imbricate fault-bend folding explains the steep southern limb of the Crêt de la Neige and the Bellecombe anticlines. 2D kinematic forward modelling yields a total amount of shortening by 23.6 km for the Western Internal Jura FTB. In addition to the primary décollement located at the base of the Keuper Group evaporites, three other décollements are found within the marly layers of the Aalenian "faciès de transition" units, the Oxfordian "Couches d'Effingen-Geissberg" members and the Berriasian Goldberg formation. The multiple thrust horizon approach is supported by new precise seismic interpretations. Our model provides a valid alternative to previous models that either propose local thickening of the Triassic evaporites or inversion of normal faults in the basement. This fully explains the elevated position of the Mesozoic cover in the Jura FTB.

Keywords Fold-and-thrust belt, Western Internal Jura, Balanced cross-section, 2D kinematic forward model, Kinematics, Geneva Basin, Thin-skinned tectonics, Shortening

1 Introduction

Studies using retrodeformation methods in the Jura fold-and-thrust belt (FTB) report shortening values up to some 30 km (Laubscher, 1965; Philippe, 1995; Affolter & Gratier, 2004), mostly achieved by thrusting and fault-related folding. These studies are based on assuming the presence of a main basal décollement horizon where all thrusts root, and on proposing a general forward propagating sequence from the internal parts towards the frontal parts. Beyond this type of geometric approach, unravelling the kinematic evolution of fold-and-thrust belts is significant to understand the geodynamic of orogenic wedges (Pfiffner, 2017; Poblet & Lisle, 2011). A particular balancing technique referred to as 2D kinematic forward modelling is a powerful tool to assess the sequence of deformation of fold-and-thrust belts. Moreover, this method reveals the geometries of the geological features for each deformation step. Recently, 2D kinematic forward models have challenged traditional

🌱 Springer Open

views in several regions in the Swiss parts of the Jura FTB (Schori et al., 2015; Nussbaum et al., 2017; Rime et al., 2019; Schori, 2021). These models have shown very different sequential developments between different areas and also highlighted the importance of secondary detachment levels. Forward stepping, as well as backward stepping propagation of thrust-related folding can be observed, sometimes in an oscillating sequence. The highly deformed Internal Jura FTB north of the Geneva Basin addressed by this study, offers an ideal setting to assess the kinematic evolution using the 2D kinematic forward modelling. Detailed tectonic observation, combined with subsurface data, provide unprecedented structural control on proposed models. In addition, geothermal prospection in the canton of Geneva (Switzerland) promoted and attracted new multidisciplinary research projects (Moscariello et al., 2020). Studies about the structural geology of the Geneva Basin focus on 2D seismic interpretations (Allenbach et al., 2017; Carrier et al., 2020; Clerc & Moscariello, 2020; Clerc, 2022; Hauvette et al., 2021), on fluid and fracture characterization (Cardello et al., 2020; Do Couto et al., 2021; Guglielmetti et al., 2022), on the stress field (Borderie et al., 2022), and seismicity (Antunes et al., 2020). All these efforts provide a wealth of information that allows for a re-assessment of the structural geology of that part of the Jura FTB that is immediately adjacent to the Geneva Basin.

The 2D kinematic forward model, proposed in this study, starts from the Geneva Basin in the SE and reaches the Bienne Valley (France), in the westernmost Internal Jura FTB, to the NW (Fig. 1a, b). A compilation of existing stratigraphic works, new harmonised geological maps, and a new tectonic map paying special attention on structural/kinematic links, all helped to construct the shallow structures of the 2D modelled cross-section. The deep structures have been constrained in the Geneva Basin and in the Western Internal Jura FTB by seismic lines converted to depth with a new velocity model. This combination made it possible to elaborate a 2D kinematic forward modelling approach. This modelling allows us to present new insight into the relative timing of the foreland deformation and thrust and fold development of the Western Internal Jura FTB (France).

2 Regional geology and tectonics

The north-western Alpine foreland includes two domains. Both domains possess a different structural style and are separated by an erosive boundary in map view: the detached Molasse Basin to the south and the strongly deformed Jura fold-and-thrust belt (FTB) to the north (Fig. 1a–c). The Jura FTB itself, can be subdivided into two distinct tectonic domains: the southwestern Internal Jura characterised by intense thrusting and folding, and the more north-westerly located External Jura, further subdivided into Plateaux zones with flat lying strata and Faisceaux zones, i.e. narrow zones of localised deformation (thrusting, folding and normal faulting) (Fig. 1a and c).

This study focuses on the western Internal Jura FTB at the north-western edge of the Geneva Basin, including large areas located in the departments of Ain and Jura within France. The Geneva Basin is part of the westernmost Molasse Basin (Fig. 1b). It is bordered to the west by the NW–SE trending Vuache strike-slip Fault including the Vuache mountain ridge, and in the south-east by the NE-SW trending Mont Salève ridge formed by a major ramp anticline (Fig. 2). From south-east to northwest, the cross-section presented hereafter crosses the summits of the Crêt de la Neige, the highest mountain of the Jura FTB with its 1720 m a.s.l., the Valserine Valley, the Crêt au Merle Mount, the Pesse Valley, and finally the Bienne River (Fig. 2). The average elevation of the Geneva Basin is around 500 m a.s.l., whereas in the Jura FTB the anticlines have elevations between 1400 and 1720 m a.s.l., and the synclines, such as the Pesse Syncline investigated here, at around 1200 m a.s.l.. This important differential topographic build-up implies substantial tectonic thickening.

2.1 Stratigraphy

A uniform stratigraphic succession for neighbouring regions (France and Switzerland) and the Geneva Basin is proposed in a new stratigraphic chart (Fig. 3). This homogenised chart summarises the compilation of regional stratigraphic works (Guillaume et al., 1972; Donzeau et al., 1997; Brentini, 2018; Charollais et al., 2006, 2007; Egal, 2007; Nagel, 2007; Rusillon, 2017; BRGM, 2020; Schori, 2021 and references therein).

In the study area, the sedimentary cover lies on top of a Pre-Mesozoic basement composed of plutonic and metamorphic rocks as well as Permian and Carboniferous continental sediments frequently found in graben systems. The oldest units of the Mesozoic sedimentary stack are of Triassic age. They were formed in a continental and restricted marine environment transgressing the Post-Variscan peneplain. The oldest Triassic Buntsandstein Group (or "Grès Bigarrés" in the study area) is composed of red coarse sandstones and conglomerates (Rusillon, 2017; Brentini, 2018). The thickness of the Buntsandstein Group is 15 m (Rusillon, 2017; Sommaruga et al., 2017). The overlying Muschelkalk Group is composed of limestones and marls separated by evaporites and dolomite layers (Anhydritgruppe). The average thickness of the Muschelkalk Group, including the Lettenkohle units (Jordan, 2016), is 135 m (Rusillon, 2017; Brentini, 2018). The uppermost Keuper Group unit shows a thickness
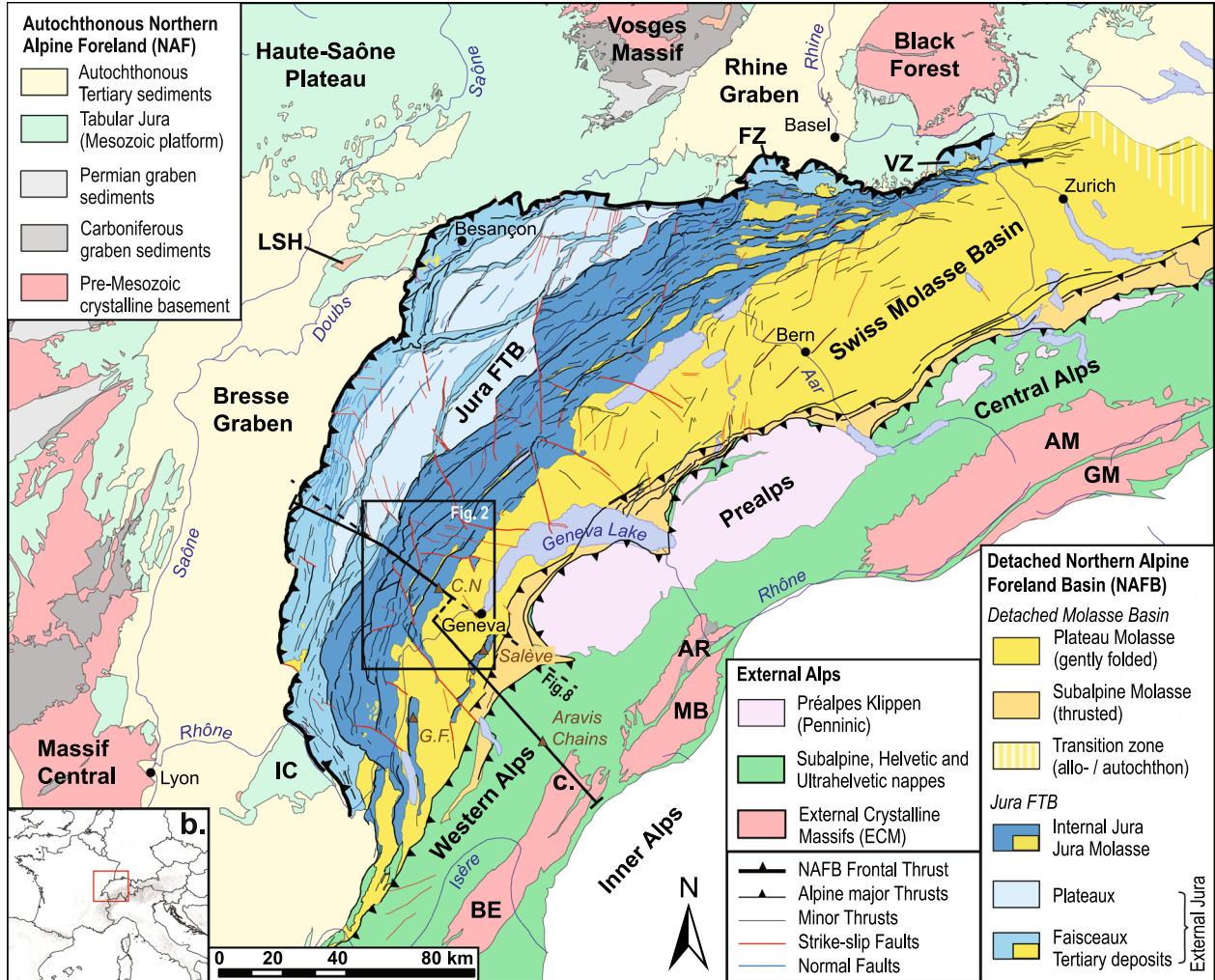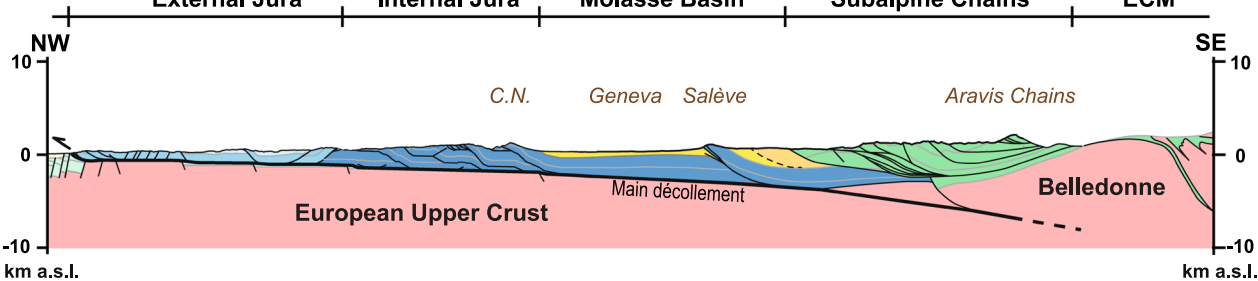
Fig. 1 Overview map of the Northern Alpine Foreland Basin (**a**) by Schori (2021) located in France and Switzerland (**b**). The tectonic units of the detached Northern Alpine Foreland Basin (NAFB) consists of the Swiss Molasse Basin (Plateau and Subalpine Molasses), the Jura Fold-and-Thrust Belt (FTB), The Ferrette Zone (FZ) and, the Vorfaltenzone (VZ). The tectonic units are fault bounded by thrusts and main faults except for the erosive boundary between the Plateau Molasse and the Internal Jura. The Autochthonous Northern Alpine Foreland (NAF) consists of: the La Serre Horst (LSH), Île Crémieu (IC), the Massif Central, the Bresse Graben, the Haute-Saône Plateau, the Upper Rhine Graben, the Vosges Massif, and the Black Forest Massif. the Prealpine Klippen, the Subalpine, Helvetic and Ultrahelvetic nappes, and the External Crystalline Massifs (ECM) including the Belledonne Massif (BE), the Mont-Blanc Massif (MB), the Aiguilles Rouges Massifs (AR), the Aar Massif (AM) and the Gotthard Massif (GM) comprise the External Alps. The study area zoomed in Fig. 2, includes the Geneva Basin and the Internal Jura. The Western Alpine transect (**c**) modified after Deville and Sassi (2006) and Schori (2021) represents the tectonic units in section view. *C.N.* Crêt de la Neige summit, *G.F.* Gros-Foug ridge

of some 300 m, and contains the "Argiles à Esthéries" and the "Grès Blonds" members (Rusillon, 2017; Brentini, 2018). The Liassic units record a marine transgression, starting with a sandy limestone (member name: "Calcaires gréseux à Chlamys") overlain by a competent limestone ("Calcaire à Gryphées" member), and marly and argillaceous limestones ("Calcaire argileux à cassure conchoïdale", "Marnes calcaires à belemnite", "Marnes à Amalthées", "Marnes noires à nodule" members) (Rusillon, 2017; Brentini, 2018). The uppermost Liassic units present a succession of limestones and marls ("Dalle échinodermique ferrugineuse", "Schistes Cartons", "Alternances micacées à bancs durs" members) (Donzeau et al., 1997; Rusillon, 2017; Brentini, 2018). The average thickness of the Liassic units is 170 m (Donzeau et al., 1997). The first Dogger unit is the 185 m thick Passwang Formation, which corresponds to the members referred to as "Faciès de transition" to the "Alternances supérieures de calcaires et marnes". The Passwang Formation is made of sandy limestones and limestones with marly alternations (Rusillon, 2017; Brentini, 2018). The overlying "Calcaires Terreux" and "Calcaires d'Arnans" members, representing the Klingnau Formation and the Ifenthal Formation, respectively, according to Rusillon (2017) and Brentini (2018), together form a 100 m thick unit. The Upper Jurassic series, mainly composed of limestone, indicate a change in the depositional environment, from deep marine to carbonate platform conditions. From the base to the top, these series are the 330 m thick Villigen-Wildegg Formation, the 245 m thick Etiollets Formation and the 130 m thick Twannbach Formation. The 30 m thick Goldberg Formation is made up of variable facies, and marks the beginning of the Cretaceous series. The overlaying Pierre-Châtel and Vions Formations form a 70 m thick unit. The upper limestones of the Chambotte Formation and the Vuache Formation have 60 m thickness. Above these units, the Grand Essert Formation has an average thickness of 100 m. The "Gorges de l'Orbe" ("Urgonien Jaune") and the Vallorbe Formation ("Urgonien Blanc", "Calcaires marneux de la Rivière" members) form one single 120 m thick unit. The only Upper Cretaceous formation preserved in the area is the "Perte du Rhône" Formation with an average thickness of 50 m. Two units of the Tertiary siliciclastic sediments are found in the study area. The Lower Fresh Molasse lies in the Geneva Basin and in the first syncline of the Jura FTB in the Valserine Valley, while the Upper Marine Molasse is only found within the Jura FTB synclines (Charollais et al., 2006, 2007). The uppermost part of the stratigraphic column are the Quaternary units which have been deposited during the last glaciation and are erosional remnants. These units are irregularly preserved and are mostly very thin and have not been distinguished in this study.

2.2 Main and secondary décollements

The deformation of the north-western Alpine foreland has long been known to be detached along a main décollement horizon, hosted in the Triassic evaporites and rooting under the frontal thrust of the basement of the External Crystalline Massifs (Buxtorf, 1907; Laubscher, 1961; Burkhard, 1990; Jordan, 1992; Philippe et al., 1996; Sommaruga, 1997; Burkhard & Sommaruga, 1998; Sommaruga et al., 2017) (Fig. 1c). This main décollement has been documented in tunnels, outcrops and drill cores (for details see Malvésy et al., 2021). All main thrusts in the Jura FTB branch off such a main décollement horizon, which is either provided by the Triassic Keuper Group in the case of the western Jura FTB or by the older Muschelkalk Group in the case of the eastern Jura FTB (Sommaruga, 1999; Sommaruga et al., 2017). Hence, in the study area, it is located in the Keuper Group (Fig. 3) as is demonstrated in the Humilly-2 deep well in the Geneva Basin (Marti, 1969; Sommaruga, 1997; Rusillon, 2017; Schori, 2021).

In addition, secondary décollements, which run over several kilometres, follow clay-rich layers and lead to a duplication of the Mesozoic cover (Laubscher, 1965; Zoetemeijer & Sassi, 1992; Noack, 1995; Medwedeff & Suppe, 1997; Schori et al., 2015; Malz et al., 2016; Rime et al., 2019). These secondary décollements are potentially following the Aalenian strata, the Oxfordian Couches

(See figure on next page.)
Fig. 2 Regional geological map of the Western Internal Jura, projected in the CH1903 + LV95 coordinates system. A succession of major, large-scale folds and ramp-flat thrusts, as well as major strike-slip faults can be recognized in the study area. Orientation of the strike-slip faults, thrusts and fold axial traces between the Vuache Fault and St-Cergue-Morez Faults are summarized in the rose diagram. The ramp-flat thrusts and the axial fold traces are oriented SSW-NNE. The strike-slip faults form a conjugate system with NNW-SSE sinistral faults and WNW-ESE dextral faults. Major dextral faults are less developed in the study area but the dextral offset is accommodated by smaller and numerous strike-slip faults forming strike-slip corridors. Oblique ramps are common in this area, per example, between the Crêt Chalam Thrust and the Vuache-Forens-Les Bouchoux (VFB) Fault. The VFB Fault and a curved Léaz-Sandézanne Axis define together a triangular zone in map view (the Léaz-Champfromier Relais) bounded in the north by the Monnetier Backthrust. The localization of the detailed geological map (Fig. 5) and the trace of the initial and final cross-sections (Figs. 7, 11) are represented by the black square and the black line. The sections cross 5 five major thrusts, from SE to NW, the Reculet Thrust, the Crêt Chalam Thrust, the Tacon Thrust and the Bienne Thrust. The section ends at the front of the Oyonnax Backthrust, which is considered to be the boundary between the Internal Jura and the External Jura (Wildi & Huggenberger, 1993). *F.* Strike-slip Fault, *T.* Thrust, *A.* Anticline, *S.* Syncline, *VFB* Vuache-Forens-Les Bouchoux Fault
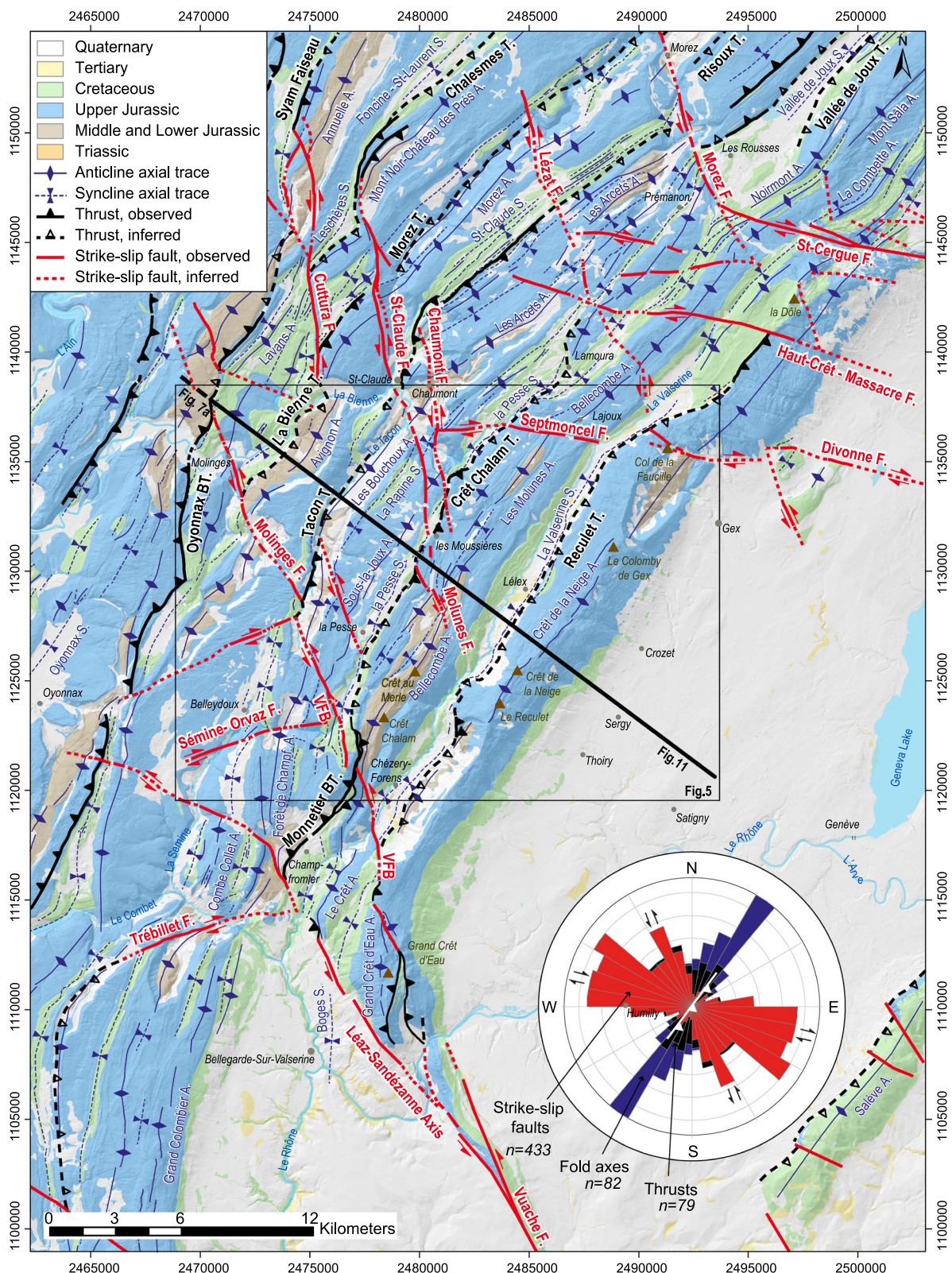
Fig. 2 (See legend on previous page.)

d'Effingen-Geissberg members, or the Berriasian Gold-berg formation (Laubscher, 1965; Endignoux & Mugnier, 1990; Philippe, 1995; Philippe et al., 1996; Schori et al., 2015; Aufranc et al., 2017; Nussbaum et al., 2017; Rime et al., 2019;) (Fig. 3). For simplicity and modelling purposes, the décollements in the 2D kinematic forward model are positioned at the base of the potential formations hosting the décollement (small arrows in Fig. 3). Accordingly, and purely for modelling purposes, the main décollement horizon that provides a broad zone of distributed deformation was located at the base of the salt rich series of the Keuper Group.

Implicitly, the Middle Triassic Muschelkalk Group series, as well as the Lower Triassic Buntsandstein Group are not included in the detached cover. They are part of the Mechanical Basement (Fig. 4). The Seismic Near-Top Basement horizon, described in this paper, corresponds to the horizon of the basement interpreted on seismic lines. The elevation of this seismic horizon contains an uncertainty of 125 m according to our new seismic interpretation (Fig. 4). The Near-Top Basement horizon includes the crystalline Basement (Basement sensu stricto), the Permo-Carboniferous sediments and probably the very thin Buntsandstein series that cannot easily be discriminated on seismic lines (Fig. 4).

2.3 Kinematics and structural geology

The arcuate Jura FTB is part of and linked to the Alpine orogeny. Most authors associate its development to the exhumation of the External Crystalline Massifs (e.g. Belledonne, Aiguilles Rouges, Mont Blanc, Aar Massifs, Fig. 1) (Buxtorf, 1907; Laubscher, 1961, 2008; Boyer & Elliott, 1982; Burkhard, 1990; Burkhard & Sommaruga, 1998) which initiated around 18 to 20 Ma (Seward & Mancktelow, 1994; Bucher et al., 2003; Leloup et al., 2005; Bellahsen et al., 2014; Boutoux et al., 2016; Ricchi et al., 2019). The Jura FTB behaves like a narrow mechanical wedge on top of a weak evaporite-rich décollement (Davis & Engelder, 1985; Sommaruga et al.,

2017). The main phase of the Jura FTB deformation has been classically set during the Miocene period according to U−Pb dating of calcite fibres (absolute timing), chronostratigraphic works, and seismic interpretations (relative timing) of the syntectonic Molasse units found in the Jura synclines (Michel et al., 1953; Rangheard et al., 1990; Deville et al., 1994; Sommaruga, 1997; Beck et al., 1998; Becker, 2000; Looser et al., 2021). The deformation of the Jura FTB is still tectonically active (Becker, 2000; Lacombe & Mouthereau, 2002; Madritsch et al., 2008) but the presently active style of deformation is a matter of debate. Based on interpretation of seismic data and suggestions that the tapered wedge is, since around some 5 Ma, no more in equilibrium, several authors have discussed a transition from an originally thin-skinned towards a thick-skinned style deformation in localised parts of the northern Alpine foreland basin (Guellec et al., 1990; Mosar, 1999; Becker, 2000; Ustaszewski & Schmid, 2007; Madritsch et al., 2008;Pfiffner, 2014;). In the Central and Eastern Internal Jura, studies on present-day seismicity argue for still on-going thin-skinned deformation, possibly decoupled from an active thick-skinned deformation (Lanza et al., 2022; Rabin et al., 2018). According to Lanza et al. (2022), the earthquakes of 2000 in St-Ursanne, of 2017 in Grenchen and of 2021 in Neuchâtel, are evidences favouring present-day thrusting located within the Mesozoic cover of the Jura FTB.

Recent chronostratigraphic and U−Pb calcite fibres dating suggest a forward stepping thrust propagation in the western and southern Jura FTB (Kalifi et al., 2021; Smeraglia et al., 2021). However, studies based on kinematic 2D forward model, absolute dating and thermochronology, argue for a complex thrusting sequence allowing for oscillating propagation sequences within the Jura FTB and the overall northern Alpine foreland (von Hagke et al., 2012; Schori et al., 2015; Malz et al., 2016; Nussbaum et al., 2017; Rime et al., 2019; Looser et al., 2021; Schori, 2021 and references therein).

(See figure on next page.)

Fig. 3 Harmonised stratigraphic chart of the Western Internal Jura FTB showing potential décollements (white arrows) and the main décollement (black arrow) based on Rusillon (2017) and Brentini (2018) (1), Strasky et al. (2016) (2), Donzeau et al. (1997) (3), Charollais et al. (2006) (4), Laubscher (1965), Philippe et al. (1996), Schori et al. (2015), Aufranc et al. (2017), Sommaruga et al. (2017), Rime et al. (2019) (5). The stratigraphic compilation allows to harmonise the existing and different geological maps of the study area and to propose a new detailed geological map (Fig. 5). This harmonisation helped to constrain and build the shallow structures in the initial cross-section (Fig. 7) through the Western Internal Jura. The stratigraphic log shows the lithologies and competences of each member, defined by the French terminology. The corresponding HARMOS formations (Fm) grouping the French members are derived from Rusillon (2017) and Brentini (2018). Uncertainties of these correspondences are specified by a question mark. The lithological legend used in the detailed geological map (Fig. 5) refers to the Harmos formations. The average thicknesses (Av. thick.) used in sections and model building are the results of a stratigraphic compilation based on well data, outcrops and stratigraphic works (Brentini, 2018; Charollais et al., 2007; Rusillon, 2017, and references therein). In the cross-sections and the 2D kinematic forward model, thin layers were grouped together (per example, c1P-V with c1G). The older lithologies have been grouped by age due to the classification uncertainty already mentioned in Rusillon (2017) and Brentini (2018). The section and model units are represented by the black separation lines. *Per.* Period, *Quat.* Quaternary, *Up-Low.* Upper-Lower Cretaceous, *Ceno.* Cenomanian, *Pliensb.* Pliensbachian, *Sine.-Hett.* Sinemurian—Hettanginian, *Alt. inf.* Alternances inférieures, *Calc.* Calcaire
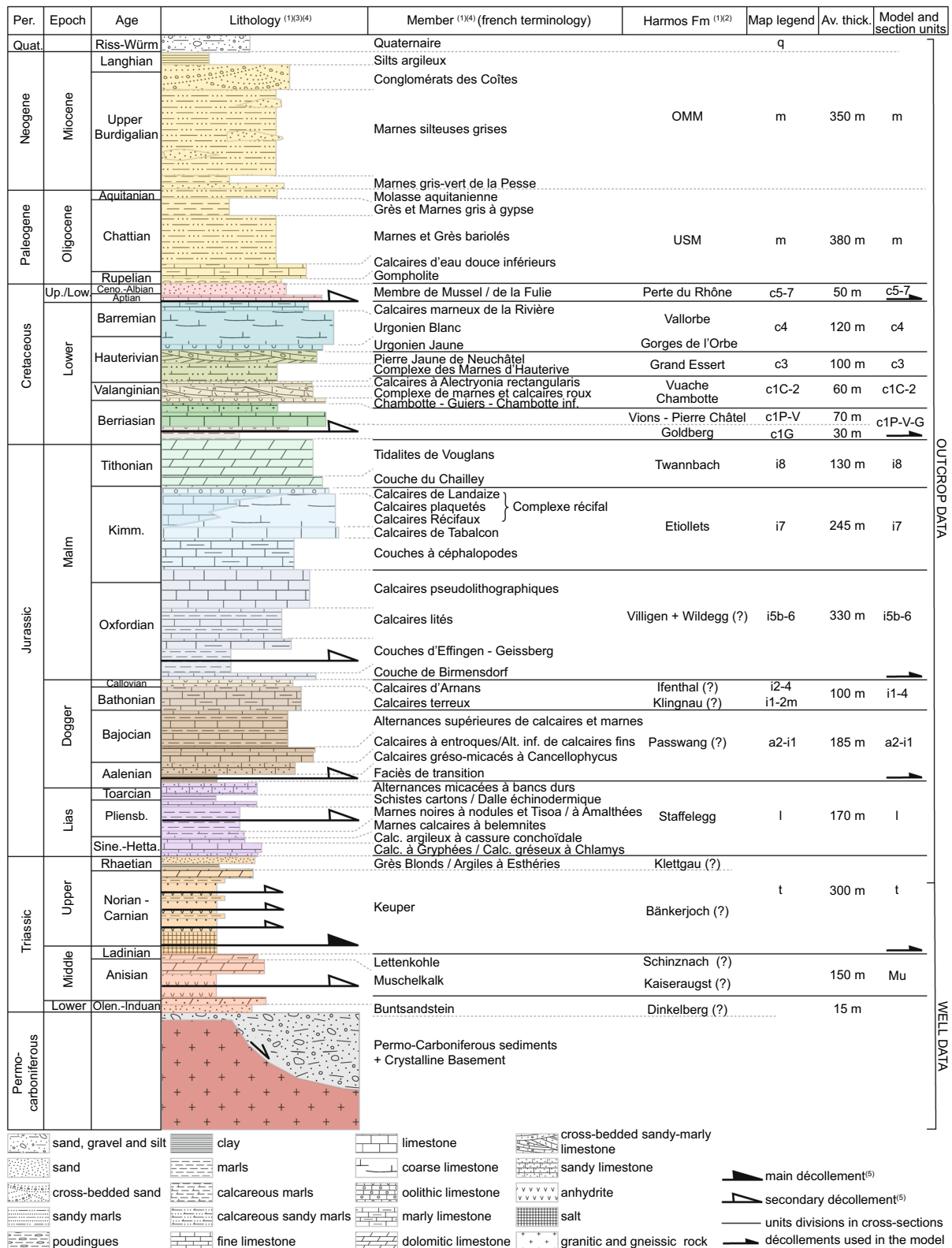
Per.	Epoch	Age	Lithology [1][3][4]	Member [1][4] (french terminology)	Harmos Fm [1][2]	Map legend	Av. thick.	Model and section units
Quat.		Riss-Würm		Quaternaire		q		
Neogene	Miocene	Langhian		Silts argileux				
				Conglomérats des Coîtes				
		Upper Burdigalian		Marnes silteuses grises	OMM	m	350 m	m
				Marnes gris-vert de la Pesse				
Paleogene	Oligocene	Aquitanian		Molasse aquitanienne / Grès et Marnes gris à gypse				
		Chattian		Marnes et Grès bariolés	USM	m	380 m	m
				Calcaires d'eau douce inférieurs				
		Rupelian		Gompholite				
Cretaceous	Lower	Up./Low Ceno.-Albian Aptian		Membre de Mussel / de la Fulie	Perte du Rhône	c5-7	50 m	c5-7
		Barremian		Calcaires marneux de la Rivière / Urgonien Blanc	Vallorbe	c4	120 m	c4
				Urgonien Jaune	Gorges de l'Orbe			
		Hauterivian		Pierre Jaune de Neuchâtel / Complexe des Marnes d'Hauterive	Grand Essert	c3	100 m	c3
		Valanginian		Calcaires à Alectryonia rectangularis / Complexe de marnes et calcaires roux / Chambotte - Guiers - Chambotte inf.	Vuache Chambotte	c1C-2	60 m	c1C-2
		Berriasian		Vions - Pierre Châtel		c1P-V	70 m	c1P-V-G
				Goldberg		c1G	30 m	
Jurassic	Malm	Tithonian		Tidalites de Vouglans / Couche du Chailley	Twannbach	i8	130 m	i8
		Kimm.		Calcaires de Landaize / Calcaires plaquetés / Calcaires Récifaux / Calcaires de Tabalcon (Complexe récifal) / Couches à céphalopodes	Etiollets	i7	245 m	i7
		Oxfordian		Calcaires pseudolithographiques / Calcaires lités / Couches d'Effingen - Geissberg / Couche de Birmensdorf	Villigen + Wildegg (?)	i5b-6	330 m	i5b-6
	Dogger	Callovian		Calcaires d'Arnans	Ifenthal (?)	i2-4	100 m	i1-4
		Bathonian		Calcaires terreux	Klingnau (?)	i1-2m		
		Bajocian		Alternances supérieures de calcaires et marnes / Calcaires à entroques/Alt. inf. de calcaires fins / Calcaires gréso-micacés à Cancellophycus	Passwang (?)	a2-i1	185 m	a2-i1
		Aalenian		Faciès de transition				
	Lias	Toarcian		Alternances micacées à bancs durs / Schistes cartons / Dalle échinodermique				
		Pliensb.		Marnes noires à nodules et Tisoa / à Amalthées / Marnes calcaires à belemnites	Staffelegg	l	170 m	l
		Sine.-Hetta.		Calc. argileux à cassure conchoïdale / Calc. à Gryphées / Calc. gréseux à Chlamys				
Triassic	Upper	Rhaetian		Grès Blonds / Argiles à Esthéries	Klettgau (?)			
		Norian - Carnian		Keuper	Bänkerjoch (?)	t	300 m	t
	Middle	Ladinian		Lettenkohle	Schinznach (?)			
		Anisian		Muschelkalk	Kaiseraugst (?)		150 m	Mu
	Lower	Olen.-Induan		Buntsandstein	Dinkelberg (?)		15 m	
Permo-carboniferous				Permo-Carboniferous sediments + Crystalline Basement				

OUTCROP DATA / WELL DATA

Legend:

sand, gravel and silt — clay — limestone — cross-bedded sandy-marly limestone
sand — marls — coarse limestone — sandy limestone
cross-bedded sand — calcareous marls — oolithic limestone — anhydrite
sandy marls — calcareous sandy marls — marly limestone — salt
poudingues — fine limestone — dolomitic limestone — granitic and gneissic rock

main décollement [5]
secondary décollement [5]
units divisions in cross-sections
décollements used in the model

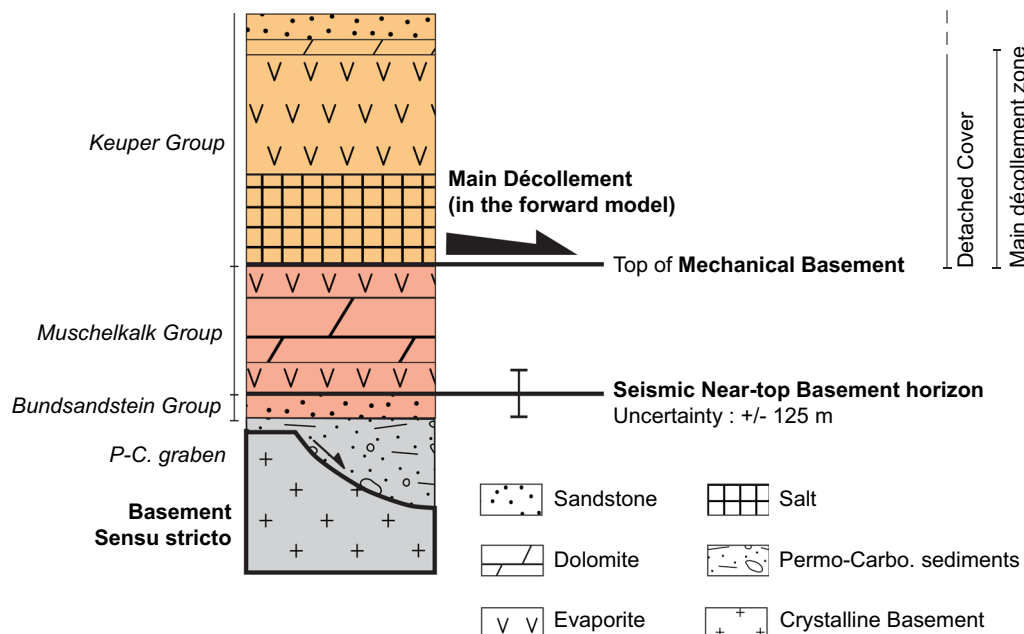**Fig. 3** (See legend on previous page.)

Fig. 4 Basement terminology and the main décollement as used in the 2D kinematic modelling approach in this paper. The Basement Sensu stricto refers to the Crystalline Basement. The Mechanical Basement is found under the cover, detached by the main décollement. In the study area, multiple minor thrusts are known to affect the Keuper Group evaporites, forming a décollement zone. For model purpose, the main décollement has been placed at the base of the Keuper Group. The Seismic Near-Top Basement as defined from seismic interpretation, is close to the top of the Buntsandstein Group with an uncertainty of ± 125 m

The shortening accommodated by the Jura FTB has been investigated in several works using retrodeformation methods (Laubscher, 1965; Philippe et al., 1996; Affolter & Gratier, 2004; Schori, 2021). For the entire Western Jura FTB (Internal and External), Affolter and Gratier (2004) calculated a shortening of 26.3 km based on map view block restoration. In the same area, Philippe (1995) and Schori (2021) calculated a shortening of 32 km, based on cross-sections balancing and map view block restoration.

In the study area (Fig. 2), a succession of major, large-scale folds and thrusts with a ramp-flat geometry can be recognised. These thrusts and the axial fold traces are on average oriented SSW-NNE (Fig. 2). The first anticlinal range of the Jura FTB is called here the Crêt de la Neige Anticline. To the north-east, this anticline shows a fault-bend fold geometry, which laterally evolves into a fault-propagation fold geometry to the south-west, with synclinal and anticlinal breakthroughs (Fig. 3). These structures are developed in the hangingwall of the Reculet Thrust which abuts against the Vuache-Forens-Les Bouchoux (VFB) Fault in the south-west (Figs. 2, 3). The Bellecombe and les Molunes Anticlines form the second range of the Internal Western Jura, and are associated to the Crêt Chalam Thrust (Fig. 2). Oblique ramps form at the transition with the VFB Fault (Fig. 3, see Donzeau et al., 1997), but also with the smaller Molunes

Fault in the centre of our study area (Fig. 2). This latter fault, although clearly located in the hangingwall of the Crêt Chalam Thrust, appears to have a continuation in the footwall unit to the north, which is offset to the north-east to form the Chaumont and St-Claude Faults (Fig. 2). The Tacon Thrust, located north-west of the Crêt Chalam Thrust, terminates in the south-west against the VFB Fault, and is offset in the north-east by the St-Claude Fault. The Chaumont Fault is restricted to the hangingwall of the Crêt Chalam and Tacon Thrusts, and terminates to the north into an oblique ramp-like segment. The Bienne Thrust, at the north-west termination of our profile, forms an oblique ramp with the Molinges Fault, and is offset by the Cuttura Fault in the north-east (Figs. 2, 3). The major Oyonnax Backthrust with its top-to-the-SE movement is situated at the north-west termination of our profile (Fig. 2). According to Wildi and Huggenberger (1993), this backthrust is the prolongation of the Syam Faisceau and is considered to form the transition from the Internal Jura to the External Plateau Jura with its narrow ribbons of higher deformation known as "Faisceaux" (Fig. 1; Laubscher, 1961; Chauve & Perriaux, 1974; Trümpy, 1980; Philippe, 1995; Sommaruga, 1997;).

Strike-slip faults, defining a conjugate fault system, contribute to compartmentalise the whole area into distinct structural domains. SSE-NNW oriented strike-slip faults are the Vuache-Forens-Les Bouchoux (VFB),

the Molinges, the Molunes, the Cuttura, the St-Claude, the Chaumont, the Lézat, and the Morez Faults (Fig. 2). They display a sinistral offset. Conjugate discrete WNW-ESE strike-slip faults (e.g. the Septmoncel Fault) are less developed in the area of investigation. In the Internal Jura, these faults show a dextral offset. In our study area, this offset is accommodated by smaller and numerous strike-slip faults (Fig. 2). To the south-west, the NW–SE oriented Vuache Fault system (bounded by the Vuache-Forens-Les Bouchoux Fault and the Léaz-Sandézanne Axis) forms a major steep, oblique ramp with a dominant sinistral strike-slip component (see Blondel et al., 1988 and Donzeau et al., 1998 for more details). It controls the structural development of the western part of the Geneva Basin and the transition to the Internal Jura FTB (Blondel et al., 1988; Donzeau et al., 1998; Wildi et al., 1991). The Molinges Fault is considered as the NNW-SSE continuation of the VFB Fault into the Jura FTB. According to seismic interpretations and absolute dating, the strike-slip faulting was coeval to the Jura thrusting and folding (Looser et al., 2021; Smeraglia et al., 2021). Strike-slip faults linked to inherited boundaries have also been reactivated during and after the deformation of the Jura FTB (Laubscher, 1961; Homberg et al., 2002; Giamboni et al., 2004; Ustaszewski et al., 2005; Schori et al., 2021;).

Published balanced and non-balanced cross-sections of the Western Jura FTB propose different interpretations of the subsurface structures (Guellec et al., 1990; Wildi & Huggenberger, 1993; Philippe, 1995; Signer & Gorin, 1995; Donzeau et al., 1998; Charollais et al., 2007; Clerc & Moscariello, 2020; Moscariello et al., 2020; Schori, 2021;). Based on the ECORS seismic line crossing the Geneva Basin and the Vuache strike-slip Fault, Guellec et al. (1990) and Philippe et al. (1996) interpreted a broad topographic high in the pre-Mesozoic basement beneath the Grand Crêt d'Eau Anticline (Fig. 2), south of our study area. Guellec et al. (1990) argue that this topographic high could either reflect the inversion of Paleozoic normal faults or a reactivation of a horst structure formed during an Oligocene extensional phase recognised in the Alpine realm. As for Philippe et al. (1996), they proposed an inversion of Permo-Carboniferous grabens. The detailed elevation map of the Pre-Mesozoic basement of Schori (2021) also shows a structural high attributable to a basement high, bound by normal faults in the Oyonnax area (Fig. 2). An alternative solution is proposed by Meyer (2000) and Cardello et al. (2020) who suggest thickening of the Triassic series at the south-eastern onset of the Western Internal Jura in order to explain the topographically higher structures. In the Western Jura FTB, north-west of our study area, Philippe et al. (1996) proposed a cross-section in the Risoux area with no inverted Permo-Carboniferous graben. Instead,

a duplication of the Mesozoic cover, with a secondary décollement is suggested, as was argued by Schori (2021), Schori et al. (2015) and Rime et al. (2019) for the northern part of the Jura FTB.

Data from hydrocarbon exploration campaigns help to constrain the deep structures. In the Geneva Basin, prior studies, based on seismic surveys have provided depth-converted seismic models of the Molasse Basin (Sommaruga et al., 2012; Clerc, 2016, 2022; Allenbach et al., 2017; Hauvette et al., 2021;), but not of the Western Internal Jura FTB. A gap of seismic data remains between the Geneva Basin and the Western Internal Jura FTB. Several seismic lines located in the study area, had not yet been converted to depth. They, are interpreted hereafter using a new velocity model.

3 Datasets and modelling

Compilation and harmonisation of the existing stratigraphic data (Fig. 3) made it possible to elaborate a new regional geological map (Fig. 2) and a new detailed geological map (Fig. 5) of the Western Jura FTB, to better constrain the surface geological structures and the regional kinematics. In addition, well data and new depth-converted seismic interpretations helped to build the deep geological structures further applied into the 2D kinematic forward model.

3.1 Stratigraphic compilaton

The section trace of this study crosses two French geological maps with different lithological legends, requiring stratigraphic harmonisation (Fig. 3). Recent harmonisation works (Rusillon, 2017; Brentini, 2018), were used to correlate and homogenise lithological units, which were previously separated in two different lithological legends from the BRGM French maps of the departments of Ain (Egal, 2007) and Jura (Nagel, 2007). The legends of the French maps (Guillaume et al., 1972; Donzeau et al., 1997; Egal, 2007; Nagel, 2007) were correlated and adapted to the swiss HARMOS legend (Strasky et al., 2016; Rusillon, 2017; Brentini, 2018;). In the French legends, some HARMOS formations have not been distinguished. Thus, the Vallorbe and Gorges de l'Orbe formations were grouped together, as well as the Vuache and Chambotte formations. For the same reason, the Pierre Châtel and Vions formations have been assembled as well as the Villigen and Wildegg formations. The older lithologies have been grouped by age due to the classification uncertainty already mentioned in Rusillon (2017) and Brentini (2018). This stratigraphic compilation was implemented into the new detailed geological map (Fig. 5).

The stratigraphic thicknesses are averages derived from existing stratigraphic works (Guillaume et al.,

1972; Deville, 1990; Donzeau et al., 1997; Charollais et al., 2006; Rusillon, 2017; Brentini, 2018) from drill-cores and databases (Charollais et al., 2007; Rusillon, 2017; Brentini, 2018; BRGM, 2020; Schori, 2021 and references therein), from wells drilled by private companies in the Pesse Syncline and, from the new wells GEo-1 and GEo-2 in the Geneva Basin (Hydro-Geo Environnement, 2018, 2020) (Fig. 3). These average thicknesses have been used for the construction of a near-surface cross-section, a 2D kinematic forward model and a final cross-section. Due to limitations of the 2D kinematic forward modelling, the thicknesses do not change along the cross-sections. Due to the scale of our model and cross-sections, The Vions-Pierre Châtel Formations have been grouped with the thin Goldberg Formation. Similarly, the Ifenthal Formation was grouped with the Klingnau Formation. The units used in the 2D kinematic forward model and the cross-sections are specified in Fig. 3 in the column "Model and section units".

3.2 Geological mapping

Based on the newly compiled stratigraphy (Fig. 3), we developed a set of harmonised maps for the Western Jura Mountains: a regional geological map (Fig. 2) and a detailed geological map (Fig. 5), which are implemented in a GIS database. We used the French harmonised vector maps of the departments of Ain (Egal, 2007) and Jura (Nagel, 2007). The limits of the geological units and the fault locations were ascertained in the study area using the digital elevation models of France (RGE ALTI V2.0) from IGN-F (2018), of Switzerland (SwissALTI3D) from Swisstopo (2011) and of the Geneva Canton SITG (2018) from SITG (2018). The bedding data have been densified with new field measurements as well as unpublished observations by David Polasek (University of Geneva). Subsequently, we derived a regional geological map (Fig. 2) where geological formations were grouped by ages (Quaternary, Tertiary, Cretaceous, Upper Jurassic, Middle-Lower Jurassic). This map contains only the major faults and the locations of the fold axes. The structures were drawn based on the dip data and morphologies observed on the digital elevation models. The naming of the main tectonic structures derives from Guillaume et al. (1972), Mudry and Rosenthal (1977), Wildi and Huggenberger (1993), Donzeau et al. (1998). The indicated strike-slip and thrusting displacements are based on geological offsets, supplemented by kinematic measurements and verified on existing maps such as the Vuache map of Donzeau et al. (1998) and the Jura tectonic map of Schori (2021).

3.3 Seismic data

The deep structures of the study area have been constrained by new interpretations of depth-converted seismic lines, based on a refined multi-layered velocity model (Table 1, Fig. 6).

We interpreted seven depth-converted seismic lines (Fig. 7a, b). In the Jura area, these lines are from 1980s surveys (JU-01, 81-JU-06, and 82-JU-18) and acquired by Celtique Energies Petroleum Ltd.. The lines 82GEX06, SJ1U3, 18SIG_003, and GG87-02 provided by the Services Industriels de Genève were used for the Geneva Basin area (Fig. 7c).

The horizons of near Base Cenozoic, Near-Top Dogger, Near-Top Keuper and Near-Top Basement, as well as the fault lines have been interpreted and picked along the two-way-traveltime (TWT) migrated seismic profiles processed in the software Kingdom version 2020. Due to the elevation differences between the Geneva Basin and the Jura FTB, as well as, the presence/absence of Molasse sediments, two different datum planes (where the TWT = 0 s) and distinct replacement velocities were chosen (Table 1, Fig. 6b).

Although there is no direct line connection between the Jura lines and the lines in the Geneva Basin, a convincing correlation could be made by comparing and correlating reflectors between the nearest seismic lines and thus adjusting for datum plane shift. The velocities used in the depth conversion are the result of the adjustment between the well data of Humilly-2 and Faucigny-1 and the seismic lines. The multi-layered velocity model applies three different velocities depending on the rheology and considers the duplication of the Mesozoic cover. This method leads to more precise depth converted profiles when compared to simpler velocity models (Fig. 6a, b). As an example, a difference

(See figure on next page.)

Fig. 5 Detailed Geological Map of the study area, projected in the CH1903 + LV95 coordinate system. Based on the stratigraphic compilation (Fig. 3), the two existing vector maps of the BRGM (Egal, 2007; Nagel, 2007) have been harmonized. Based on Rusillon (2017) and Brentini (2018), the lithological legend, used here, follows the swiss HARMOS formations. New dip data from fieldwork and wells used for building the cross-section have been located on the map. The wells names are the: GEo-1, L-112, SPM-1, SPM-2, SPM-3, G1, F1, F2, F3. This resulting harmonization helped to well constrain the surface structures of the initial cross-section (Fig. 7). The bold black line corresponds to the initial and the final cross-section of this study (Figs. 7, 11). The section trace with a calculated best-fit orientation crosses four major thrusts (Reculet, Crêt Chalam, Tacon and Bienne Thrusts) and ends in the north-west at the front of the Oyonnax Backthrust. The cross-section avoids the major strike-slip faults in order to have a balanced kinematic 2D forward model
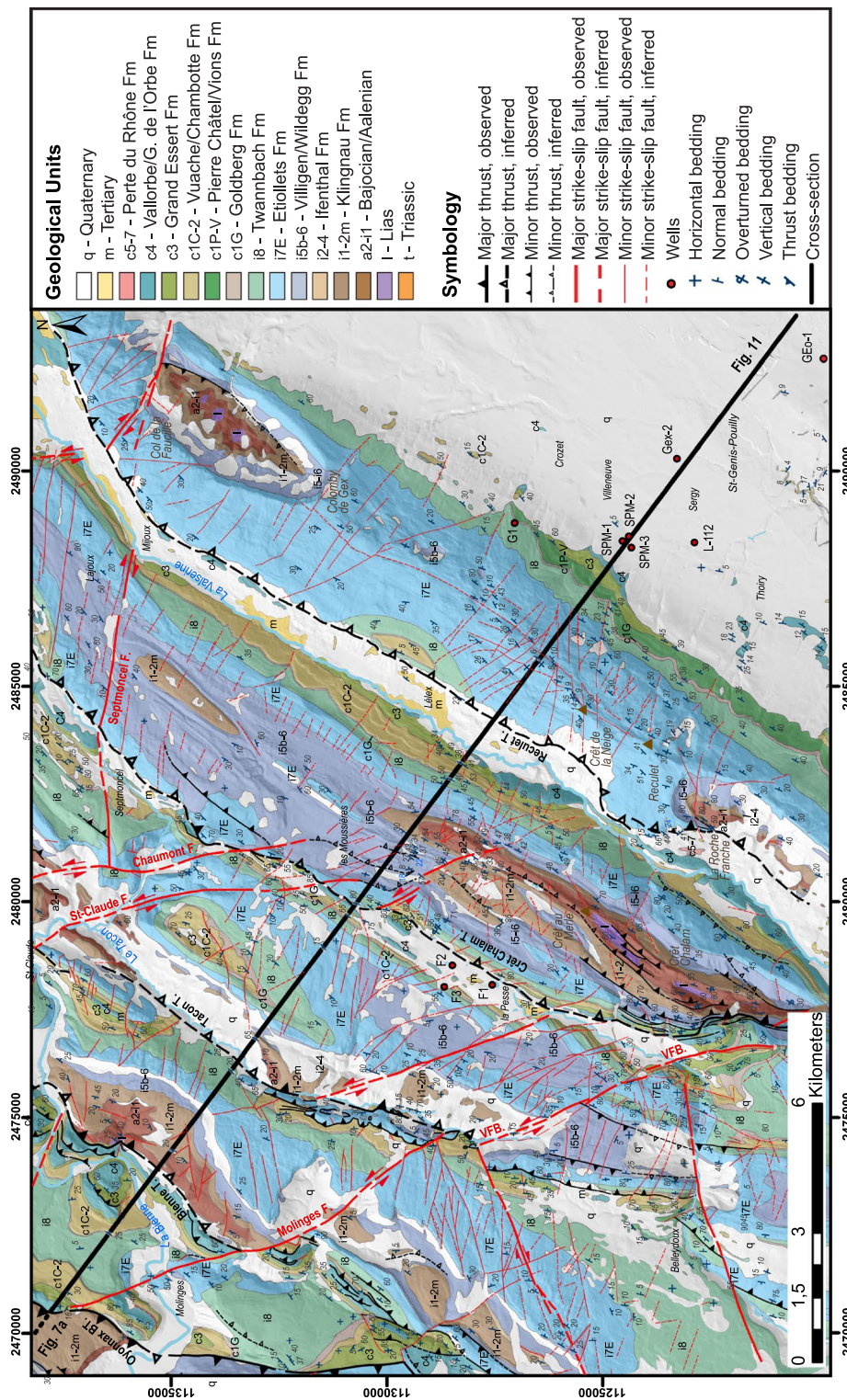
Fig. 5 (See legend on previous page.)

Table 1 Table of the conversion velocities of the new multi-layered velocity model

Seismic lines	SRD [m a.s.l.]	Stratigraphic intervals	Velocity [m/s]
Jura lines	1125	From SRD to Topography	4500
		Cenozoic	–
		Cretaceous	5340
		Malm	5340
		Dogger	4520
		Lias	4520
		Triassic	5101
		Basement	5000
Geneva lines	500	From SRD to Topography	3000
		Cenozoic Upper Part	3000
		Cenozoic Lower Part	4000
		Cretaceous	5340
		Malm	5340
		Dogger	4520
		Lias	4520
		Triassic	5101
		Basement	5000

SRD Seismic Reference Datum. Two different SRD have been applied for the Jura domain and the Geneva Basin because of the elevation difference and the absence or poorly amount of Cenozoic sediments in the Jura Mountains. The conversion velocities derive from the adjustement between well data and seismic lines

of 50 m at the Near-Top Basement horizon on the Jura lines has been measured between a one-layer velocity model and the multi-layered models (Fig. 6c).

The seven depth-converted seismic profiles with their interpretations have been projected parallel to the regional fold axial trend (axis oriented N35°) into the initial cross-section (Fig. 7a, b).

3.4 2D kinematic forward modelling

We used a 2D kinematic forward modelling approach to obtain a geometrically viable and balanced cross-section and to propose a kinematic evolution of the Western Internal Jura FTB. When applying the fault-related fold theory (Brandes & Tanner, 2014; Suppe, 1983, and references therein), this method does not only yield the shortening induced by the thrusting and folding, but

also gives a kinematically viable sequence of deformation. The methodology is based on the strategies proposed by van Mount et al. (1990) and Nussbaum et al. (2017). Compilations of all existing data allow us to construct an initial hypothesis about the fold and fault geometries. This compilation subsequently helps to constrain a 2D kinematic forward modelling (Figs. 9, 10) as developed in the software Move^tm version 2020.1 by Petroleum Experts. The trace of the 2D kinematic forward model is oriented parallel to what is considered the main regional tectonic transport direction (generally taken as perpendicular to fold axial orientations and direction of main thrusts) and avoids the major strike-slip faults. Therefore, the movements in and out of the section is kept minimal and the model remains balanced.

The tool "2D-Move on fault" displaces the sedimentary cover and pre-existing structures with different algorithms above a given fault geometry. The Fault-Bend Fold (Suppe, 1983), the Trishear (Erslev, 1991; Allmendinger, 1998; Hardy & Allmendinger, 2011) and the Fault-parallel Flow (Egan et al., 1997; Ziesch et al., 2014) algorithms were used to forward model the hanging wall geometries at the top of a pre-defined fault. We used the Fault-bend-Fold algorithm to build the folds developing above flat-ramp-flat thrusts. The Trishear algorithm has been applied to develop the frontal limb of the folds and, the Fault-parallel flow has been used above complex fault geometries.

Starting with an initial stage, the concept of secondary décollements (Schori et al., 2015; Nussbaum et al., 2017; Rime et al., 2019) and hypotheses about flat-ramp thrusts geometries have been tested iteratively in order to find viable solutions. During each iteration, we compared the modelling geometries with the near-surface cross-section. The fault geometries and the displacements have been adapted until the 2D kinematic forward model fitted with the shallow geological features (Fig. 7c).

4 Surface and seismic interpretations

The interpretation of the near-surface and deep geological structures of the Western Internal Jura have been reassessed by updating and reprocessing the surface and seismic data. These results help to constrain and validate the 2D kinematic forward model.

(See figure on next page.)
Fig. 6 Differences between the single layer velocity model **A** and the multi-layered velocity model **B** on the seismic lines 81-JU-06 and 80-JU-01. The seismic traces are localized on Fig. 7. The multi-layered velocity model considers the duplication of the Mesozoic cover by applying three different velocities depending on the rheology. This method allows to have a more precise depth-converted seismic lines than simple conversion model and to well constrain the elevation of the horizons. **C** The seismic lines have been converted into depth by the multi-layered velocity model. 50 m depth difference is observed at the Near-Top Basement horizon between the two models (**B**). In this study, the more precise multi-layered velocity model has been used to interpret the seismic lines in the vicinity of the cross-section (Fig. 7). The major thrusts (Crêt Chalam, Tacon and Bienne Thrusts) have been built in the kinematic 2D forward model. *Topo* Topography horizon, *NTDo* Near-Top Dogger horizon, *NTKeu* Near-Top Keuper horizon, *m.d.* main décollement, *NTBas* Near-Top Basement, *InPal* Intra-Paleozoic
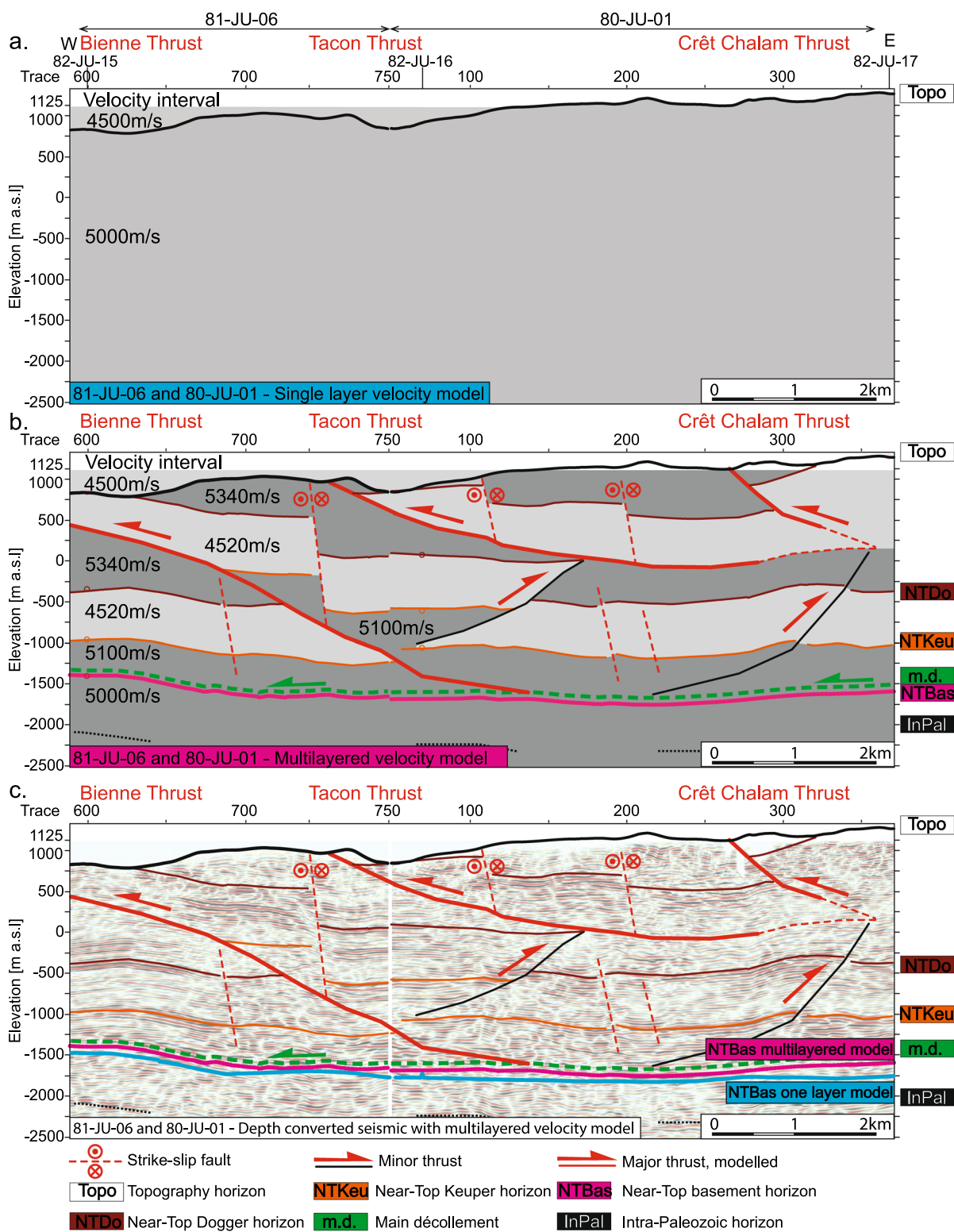
Fig. 6 (See legend on previous page.)

4.1 Seismic interpretations

In the Geneva Basin, flat reflectors, such as visible on the GG87-02 line, are offset by subvertical faults (Fig. 7b). Imbricates or/and thickening are also observed in the Keuper Group. At the north-western front of the Geneva Basin, reflectors are observed under the seismic Near-Top Basement on the SJ1U3, GG87-02, 18SIG_003, and 82GEX06 lines (Fig. 7b). On the southern flanks of the Crêt de la Neige Anticline, reflectors of SJ1U3 and 82GEX06 lines dip towards the south-east and subvertical faults or SE-verging thrusts cut the entire Mesozoic cover. In the same area, the Near-Top Basement horizon shows small steps on the SJ1U3 line.

In the Jura FTB, under the Bellecombe Anticline, the reflectors of the 82-JU-18 and 80-JU-01 highlight the duplication of the Mesozoic cover and therefore, the flat-ramp geometry of the Crêt Chalam Thrust (Figs. 6, 7b). Below this thrust, we interpreted deep SE-verging thrusts, folds in the Dogger units, and imbricate structures in the Keuper Group. The Bienne Thrust is visible on the 81-JU-06 line, north-west of the Tacon Thrust. Towards the west, the pop-up structure on the 81-JU-06 line (Fig. 7b), which is offset on the cross-section, represents the Oyonnax Syncline located west of the study area (Fig. 2) and its SE-verging backthrust.

4.2 Near-surface cross-section

A non-balanced, near-surface cross-section (Fig. 7c) including our new surface investigation, has been built in order to better constrain the surface geometries of the 2D kinematic forward model, and to serve as a control section.

In the Geneva Basin, the surface dip data and the data of GEo-1 well suggest a large, low-amplitude anticline (Fig. 7c). At the north-western edge of the basin, folds may be associated with south-verging reverse faults, interpreted on the lines SJ1U3 and 82GEX06 and supported by the L-112 drillcore showing a highly fractured zone, indicated by steep dip measurements (Charollais et al., 2007).

Along the south-eastern foothill of the Crêt de la Neige Anticline, the Cretaceous strata dip 25° towards the south-east, as measured in the SPM-1, SPM-2, SPM-3 drillcores, located at the anticline ramp (Charollais et al.,

2007). Further north, at higher elevation, steeper beddings (between 40° and 60°) suggest a bend that may be related to the Reculet Thrust at depth. Molasse units are outcropping in the Valserine Syncline. The Reculet Thrust and its secondary branches breach the surface along the meridional side of the valley, as can be seen in the La Roche Franche outcrop (Fig. 5). Here, reverse and steep bedding reveal an inverted anticlinal limb in the hanging wall of the Reculet Thrust. To the north-east, a small syncline of Cretaceous units near the town of Lélex (Fig. 5) is also located in the hanging wall. Thus, the two branches of the Reculet Thrust represent synclinal and anticlinal breakthroughs. The following Bellecombe Anticline initiates at the north-west side of the Valserine Valley (Fig. 7c). At the top of the anticline, the Dogger units reach the surface and exhibit a series of metric to decametric minor folds within the fold core. In the valley of Les Moussières (Fig. 5), at least three secondary thrust faults have been observed and are interpreted to root in the flat of the Crêt Chalam Thrust. These imbrications have also been mapped in the south-west by Donzeau et al. (1997) near the Crêt Chalam Mount. They typically are associated with small folds composed by Dogger and the Oxfordian units seen on the field. South of Les Moussières area, the Crêt Chalam Thrust and its imbrications form oblique ramps with the Molunes strike-slip Fault (Figs. 2, 5). In the area of the section trace, the main Crêt Chalam Thrust overrides the Pesse Syncline and completely covers the Molasse units.

Similarly to the cross-section proposed by Charollais et al. (2006), the Pesse Syncline is considered as a box fold in agreement with the steep beddings measured north-west of the valley (Fig. 5). The subvertical beddings rapidly turn horizontal and then gently dip to the northwest to form a syncline in the hanging wall of the Tacon Thrust to the north (Fig. 7c). Following the suggestion of Wildi and Huggenberger (1993), the hanging wall of the Tacon Thrust is related to a shallow structure. Indeed, a shallow flat of the Tacon Thrust north of the Pesse Syncline is required to bring the Dogger and Liassic units to the surface (see also Philippe, 1995; Schori, 2021). The Tacon Thrust overrides the Cretaceous layers forming the folded hanging wall of the north-westerly adjacent

(See figure on next page.)

Fig. 7 Near-surface cross-section with seismic interpretations. The cross-section derives from surface and well data. The section trace crosses the Reculet Thrust, the Crêt Chalam Thrust with its imbrications, the Tacon Thrust, the Bienne Thrust and terminates in the north-west at the front of the Oyonnax Backthrust. The seismic lines have been converted with the new multi-layered velocity model (Fig. 6b). These seismic-depth interpretations allow to position the horizons and the faults with more precision than simpler conversion models. The interpreted horizons and reflectors of the seismic lines 81-JU-06, 82-JU-18, SJ1U3 and GG87-02 (**b**) have been projected on the initial cross-section (**a**) parallel to the regional fold axial trend (N35°). The interpretations of the 81-JU-06 seismic line are offset due to the projection. A gap of seismic data exists between the Geneva Basin and the Valserine Syncline. Despite this gap, the initial cross-section (**a**), the seismic horizons and interpreted faults and thrusts (**b**) helped to have an insight of the deep structures with good accuracy for the forward modelling. The cross-section (black straight line) the wells (red dots) and seismic lines (in black) are located on the small map (**c**). *T.* thrust, *B.-T.* backthrust, *S.* syncline, *A.* anticline
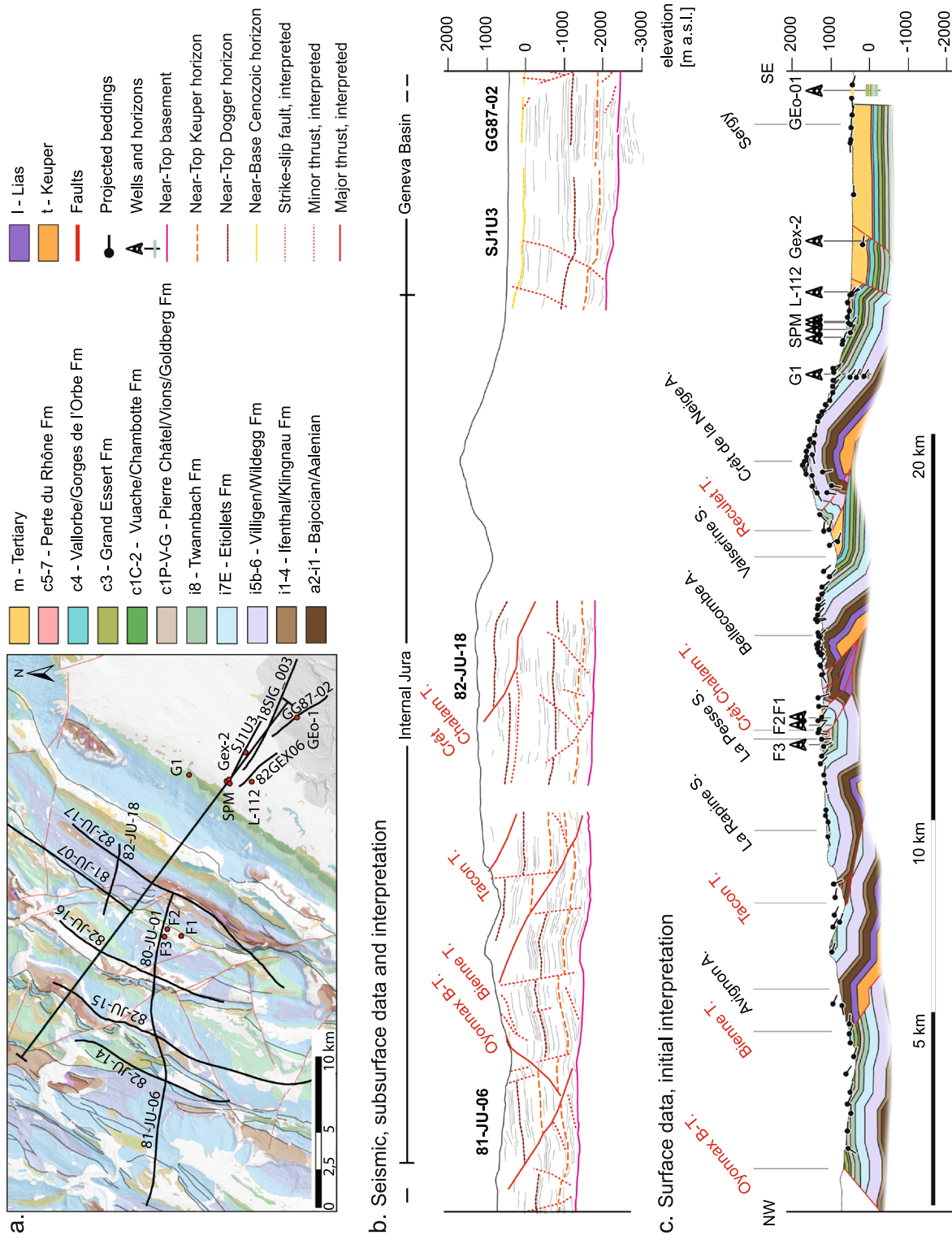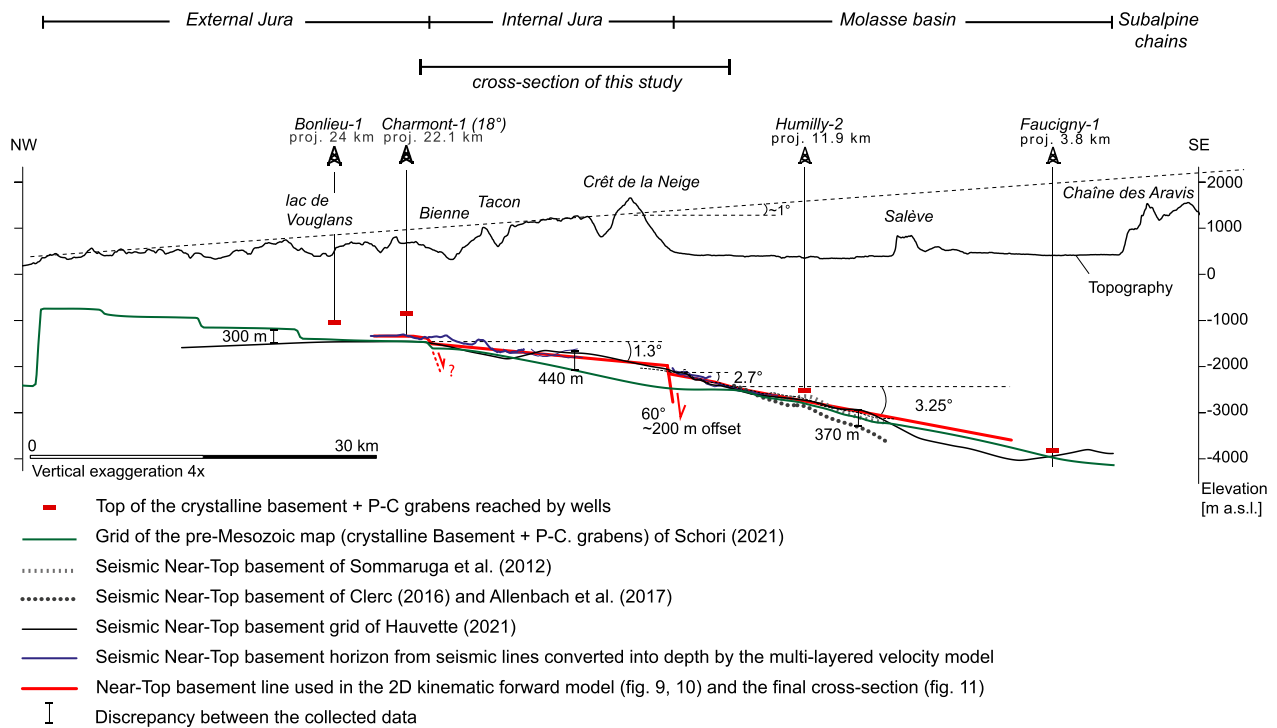
Fig. 7 (See legend on previous page.)

Fig. 8 Transect of the Near-Top Basement line used in the 2D kinematic forward model compared with existing data. This transect is located in Fig. 1. Comparisons between well data and different seismic and elevation models (Sommaruga et al., 2012; Clerc, 2016; Allenbach et al., 2017; Hauvette et al., 2021; Schori, 2021) have been performed to have the most precise elevation of the Near-Top basement horizon for the 2D kinematic forward model. The Near-Top basement line used in this study (black bold line) follows the seismic interpretations of Hauvette et al. (2021) and grids converted by the new multi-layered velocity model. These data are compared with other studies by indicating the discrepancy between them. The highest difference (400 m) is situated beneath the Crêt de la Neige, where no seismic data has been recorded. The top of the basement under the Jura FTB dips more gently than under the Geneva Basin. We interpret this change in angle as a preexisting normal fault with a supposed offset of 200 m beneath the SE flank of the Crêt de la Neige

Bienne Thrust. No Tertiary Molasse series are known in the footwall of the Tacon Thrust.

4.3 The Near-Top Basement horizon
The location of the Near-Top Basement horizon (Fig. 8) is based on our new seismic interpretation, and on existing data compilations (Sommaruga et al., 2012; Clerc, 2016; Allenbach et al, 2017; Hauvette et al., 2021; Schori, 2021).

Comparisons between different published seismic and elevation models have been performed in order to assess the elevations of the Near-Top basement horizon. The elevation of the Near-Top Basement horizon used in the 2D kinematic forward model (Fig. 8) is based on a combination of various sources of information. These comprise:

- the Pre-Mesozoic basement map of Schori (2021);
- well data (Humilly-2 and Faucigny-1);
- the seismic lines converted into depth by our new multi-layered velocity model;
- the 3D seismic models, which are the horizons grids from Hauvette et al. (2021), from the GeoMol (Clerc, 2016, 2022; Allenbach et al., 2017), and finally also

from the seismic Atlas of the Swiss Molasse Basin (Sommaruga et al., 2012).

Between the wells of Faucigny-1 and the Humilly-2, the average slope of the Near-Top Basement contact is tilted by 3.3° towards the south-east (positioning uncertainty of 150 m, Fig. 8). The dip changes to 2.7° between the well Humilly-2 and the northern end of the Geneva Basin. In the latter area, the Near-Top Basement horizon reaches an elevation of − 2200 m a.s.l.. Beneath the Crêt de la Neige Anticline, no seismic data are available. Between the Pesse Syncline and the Bienne Valley, the Near-Top Basement horizon dips at about 1.7° towards the south-east at an elevation respectively between − 1900 m a.s.l. and − 1300 m a.s.l.. A possible basement step interpreted by Schori et al. (2021) is located in the area north-west of the Bienne Thrust. Following the work Schori (2021) and Schori et al. (2021), the change in angle between the Geneva Basin and the Jura FTB domain, located approximately under the south-eastern flank of the Crêt de la Neige Anticline, is considered to be linked to a pre-existing normal fault in the basement, with a supposed offset

of 200 m (Fig. 8). This well constrained Near-Top basement horizon allows to build with precision the elevation of the Mesozoic cover in the 2D kinematic forward model and the final cross-section.

5 2D Kinematic modelling results

Based on stratigraphic compilation, new maps, seismic interpretation, near-surface cross-section, new interpreted Near-Top Basement horizon, we developed a 2D kinematic forward model (Figs. 9, 10) resulting in a balanced cross-section (Fig. 11) between the Geneva Basin to the Bienne Valley.

5.1 Kinematic evolution of the Western Internal Jura FTB

Following a series of successive iterations, the best-fit 2D kinematic forward model (Figs. 9, 10) has a thin-skinned deformation style with multiple secondary décollements. This solution proposes that the Western Internal Jura FTB is built up by 4 major thrusts, which all show a complex fault geometry and a forward stepping deformation. In addition, these major thrusts are reactivated partly by back-stepping sequences of thrust imbricates. The transition of the future Molasse Basin – Jura FTB is characterised by a step in the basement surface. This 2D kinematic forward model yields a total of 23.6 km shortening from the Geneva Basin to the Bienne Valley.

The initial stage shows the Alpine foreland basin prior to folding and thrusting. The first deformation initiates with the Reculet flat-ramp Thrust rooting in the Keuper Group (Fig. 9, step 1). This thrusting displaces the Mesozoic cover of 4.5 km towards the north-west and forms the initial Crêt de la Neige Anticline. The second displacement reactivates this flat-ramp thrust and develops an imbricate. Both deformations result in the synclinal breakthrough, observed east of the town Lélex, in France (Fig. 9, step 2). Then, the north-westerly adjacent Crêt Chalam Thrust is initiated 10.6 km further north from the tip of the Reculet Thrust (Fig. 9, step 3). It develops a series of 3 ramp-flat segments. The deepest ramp segment of the modelled Crêt Chalam Thrust shows a dip of 25° and ramps from the Keuper Group evaporites into the Faciès de Transition units of the lower Aalenian age. The following 3 km long flat elevates and preserves the Valserine Syncline below the Reculet Thrust. At the end of

this buried flat, the Crêt Chalam Thrust is characterised by another ramp segment. Then, the thrust follows a secondary décollement located at the base of the Cretaceous Goldberg Formation, before reaching the surface. On the shallowest flat of the Crêt Chalam Thrust, four back-stepping imbrications raise the Dogger and Liassic units lying nowadays at more than 1200 m a.s.l. in the core of the Bellecombe Anticline (Figs. 9, 10, steps 4–7). The Crêt Chalam Thrust and its imbrications accommodate 6.4 km of shortening. Due to the imbricate fault-bend folding, the Reculet Thrust has been passively deformed above the Crêt Chalam Thrust. The next, younger Tacon Thrust (Fig. 10, step 8) initiates in the Keuper Group 12.5 km in front of the tip of the Crêt Chalam Thrust. This flat-ramp-flat thrust follows the secondary décollement in the Effingen marls for 3.2 km to elevate and preserve the Pesse Syncline between the Tacon and the Crêt Chalam Thrusts. At the end of this flat, the Tacon Thrust forms a ramp and develops another flat in the marly layers of the Goldberg Formation. The Tacon Thrust accommodates a shortening of 8.2 km. Like the Reculet Thrust, the Crêt Chalam Thrust is passively deformed above the Tacon Thrust due to the imbricate fault-bend folding. On the shallow flat of the Tacon Thrust, a south-verging thrust explains the steep beddings measured on the north-west flank of La Pesse Syncline (Fig. 10, step 9). Finally, the Bienne Thrust (Fig. 10, step 10) starts 11.5 km in front of the tip of the Tacon Thrust. A displacement of 3.4 km was necessary to raise the Dogger and Liassic units to the surface, as observed in the field. The formation of small imbricates in the Keuper Group are required to explain the Triassic thickening and the folds observed on seismic lines (Figs. 7b, 10, step 11).

5.2 Final cross-section

The final cross-section (Fig. 11) is a kinematically and geometrical viable section of the Western Internal Jura, from the Geneva Basin to the Bienne Valley, with deep structures validated by 2D kinematic forward modelling (Figs. 9, 10).

The multiple thrust horizon model, in addition to the main décollement is in agreement with the structurally and topographically higher position of the Valserine

(See figure on next page.)
Fig. 9 Part 1 of the 2D kinematic forward model from the Geneva Basin to the Bienne Valley (deformation steps 0 to 5). In the individual deformation steps, the active thrust is shown in black and inactive thrusts are coloured in red. The numbering of the faults corresponds to the sequence of deformation. Step 0 corresponds to the Northern Alpine Foreland stage prior to the Jura thrusting and represents the initial layer cake model supplemented by the information about the basement depth (Fig. 8). Step 1 indicates the first deformation and step 11, the last one. The Mesozoic cover shown in the forward model, has been built on the Near-Top Basement line (Fig. 8). The 1st and 2nd deformation steps the folding of the Crêt de la Neige Anticline related to the movement along the Reculet Thrust. The steps 3 to 5 show the movement along the Crêt Chalam Thrust with its imbrication, leading to the Bellecombe Anticline. The algorithm used in Move^tm version 2020.1 with the resulting shortening is detailed for each step
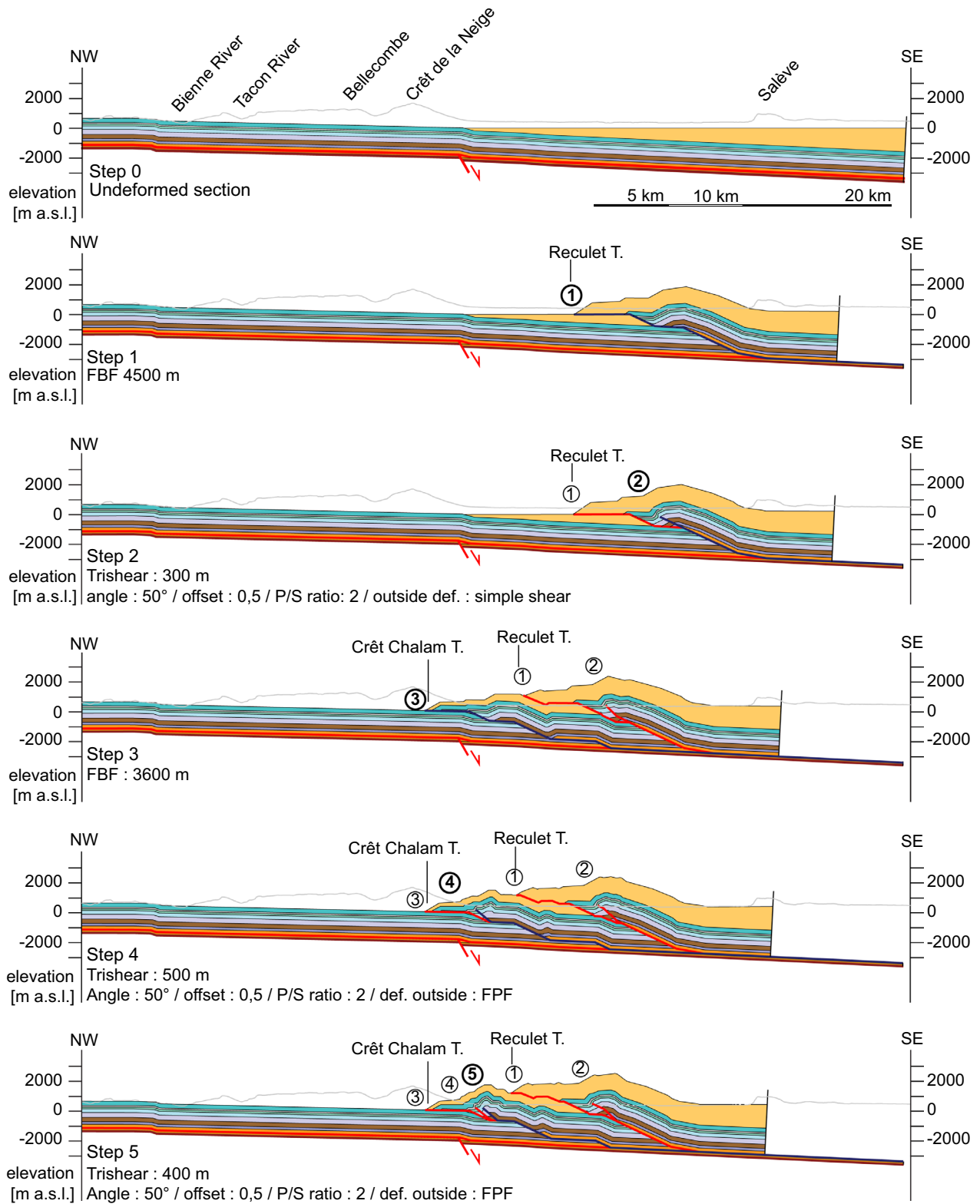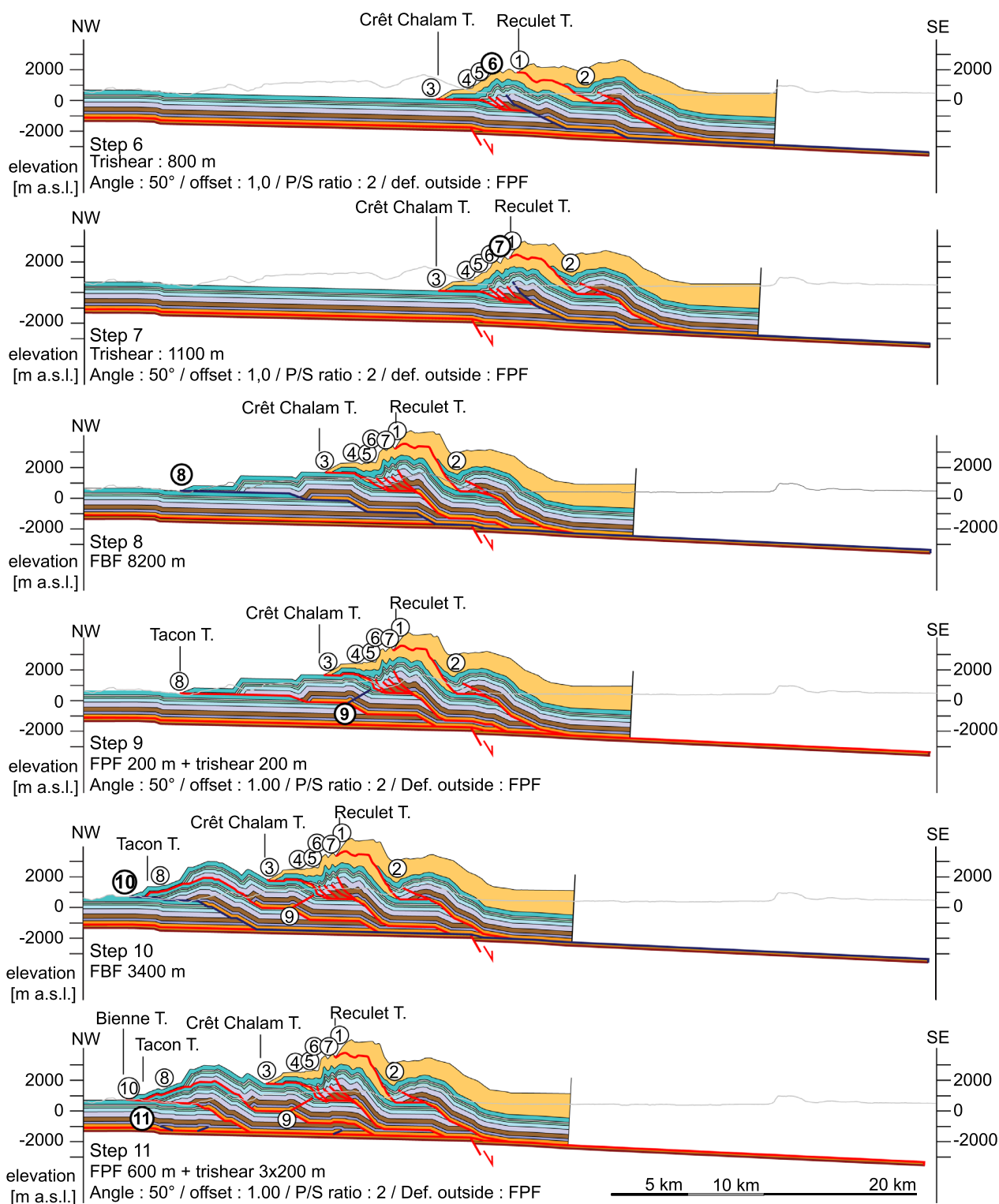
Fig. 9 (See legend on previous page.)

Fig. 10 Part 2 of the 2D kinematic forward model from the Geneva Basin to the Bienne Valley (steps 6 to 11). Step 6 to 7 show the last imbrications of the Crêt Chalam Thrust. The step 8 and 9 are attributed to the Tacon Thrust and the smaller Tacon Backthrust. The Bienne Thrust is initiated at step 10. At the last step (11), we added Triassic thickening under the Jura FTB. The Triassic thickening is poorly time constrained (see discussion for more details). The lithological legend can be found on Fig. 11
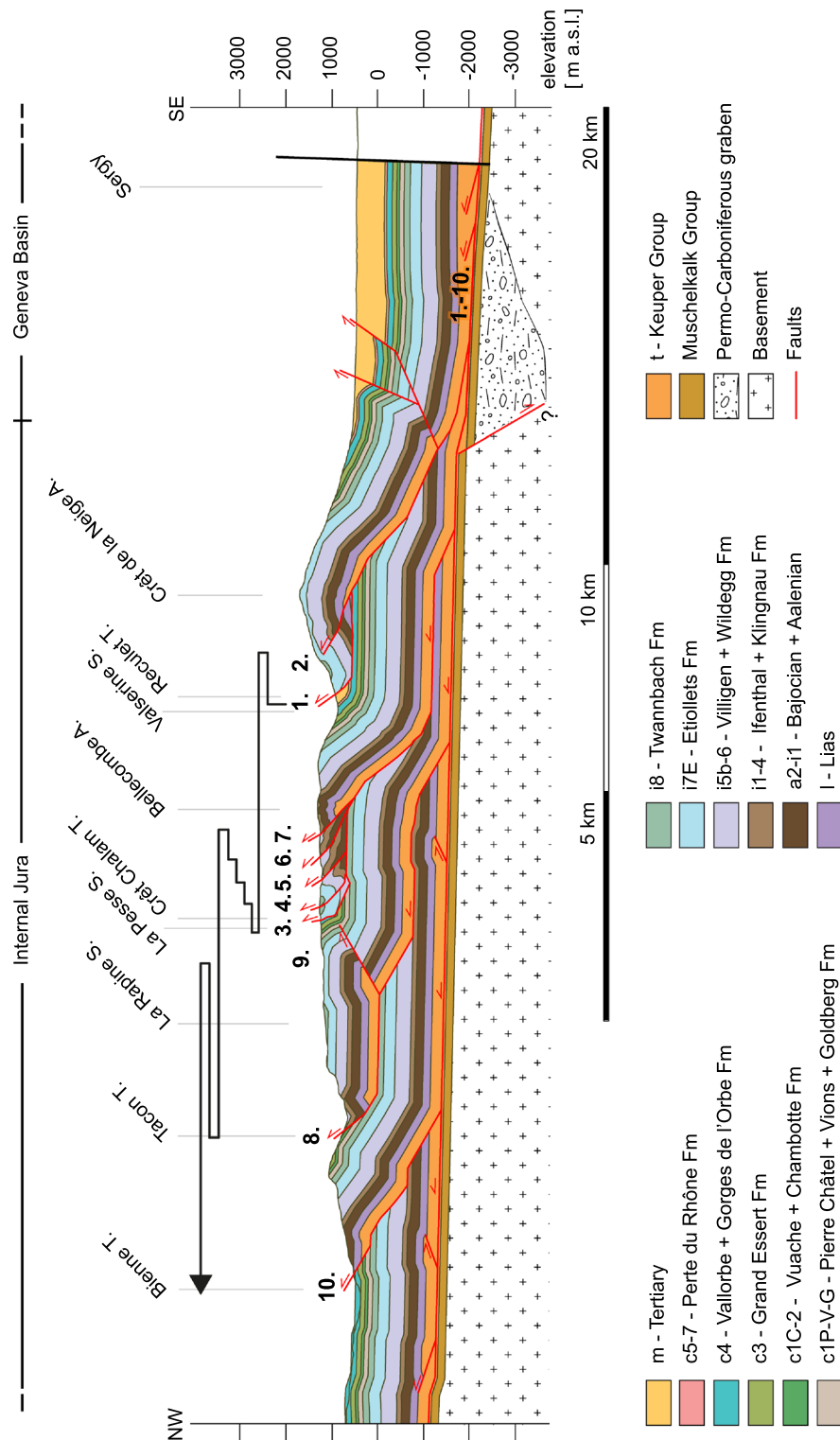
Fig. 11 Final balanced cross-section from the Geneva Basin to the Bienne Valley. The section trace is located in Figs. 1, 2, 5 and 12. The surface structures are constrained by the near-surface cross-section while the deep structures are based on the seismic data (Figs. 7, 8) and the 2D kinematic forward model (Figs. 9, 10). Due to model limitations, some geological features have been modified or added to the section, such as the subvertical faults, the Triassic thickening and, the Permo-Carboniferous graben in the Geneva Basin. The numbers on top of the thrusts (in red) indicate the chronology of thrusting activity. The main décollement located at the base of the Keuper Group has been active during the all deformation. This sequence illustrated by the black arrows shows a forward stepping deformation accompanied by minor back-stepping thrust sequences. This multiple thrust horizon approach is an alternative to the thick evaporitic duplexes or basement highs solutions

Syncline, the Bellecombe Anticline, the Pesse Syncline and, La Rapine Syncline (see Fig. 2).

Due to model limitations, minor modifications of the final step of the 2D kinematic forward model have been done to match the surface structures of the initial non-balanced cross-section, the well data and, the seismic interpretations as closely as possible. These minor adjustments are presented on the final cross-section (Fig. 11). Since the horizons observed on the well GEo-1 well are in a higher position (Fig. 7b) than in the proposed model (Fig. 10), simple imbricates have been drawn within the Keuper Group under the Geneva Basin in order to elevate the overlying Mesozoic cover. In the southern foothill of the Crêt de la Neige anticline, we added two south-verging reverse faults observed on the seismic lines SJ1U3 and 82-GEX06 and the shallow well L-112 (Fig. 7a). The solution provided by the 2D kinematic forward model suggests a longer flat of the Crêt de la Neige Thrust compared to the near-surface cross-section. The longer flat allows to have a balanced anticline fitting with the dip data and the geological outcrops. The fold limbs in the hanging wall of the Reculet Thrust have been slightly modified in the final cross-section to respect the dip data measured in the field. The 2D kinematic forward model proposes an additional imbrication of the Crêt Chalam Thrust. This imbrication allows to create a fold limb observed in the field at the front of the Crêt Chalam thrust. The structures inside these imbrications, as well as the south-eastern hinge of the propagation fold above the south-verging Tacon Backthrust, have also been adjusted to the dip data measured in the field (Fig. 5). The modelling and balanced solution concerning the geometry of the Tacon Thrust front shows, that the Dogger units do not need to be tectonically duplicated as it has been drawn initially on the near-surface cross-section.

6 Discussion

6.1 Modelling limitations and modifications in the final cross-section

The precision of the 2D kinematic forward model, allowing to resolve some of the finer details in the structural geometry, is limited by the algorithms and the scale of the cross-section. We need to consider that the structures produced by these algorithms have simple and idealised geometries. They should be more complex in nature (see Butler et al., 2018 for more details). The scale of the model allows to construct the main thrusts and folds, but

it does not allow to consider minor faulting and folding. Moreover, the software only uses predefined thrusts, and thus does not create new faults that may be otherwise induced by the thrusting and folding. The stratigraphic thicknesses are constant in the 2D kinematic forward model. However, this does not mean that changes of lithological thickness are not present in the region.

For these reasons, we modified the last minor step of the 2D kinematic forward model in certain areas in order to better fit the structures observed on the field and interpreted on the basis of non-balanced cross-sections and of seismic lines (Fig. 7). The final cross-section (Fig. 11) results from such minor adjustments.

The Triassic thickening observed in seismic data underneath the Jura FTB and the Geneva Basin has been modelled during the last stage of our model but in this regard the sequence of deformation remains hypothetical. In fact, the existing data do not permit to constrain the timing of the deformation within the Triassic series of the Keuper Group imbricates nor eventual thickening. However, the Keuper Group imbricates/thickening modelled do have an influence on the folding geometries (Fig. 10). The imbrication of Triassic series beneath the flat of the Crêt Chalam Thrust (Fig. 11) may explain folds observed in seismic lines (Fig. 7b). In the same area, the seismic interpretation shows south-verging faults to explain the minor offset of the seismic horizons (Fig. 7b). In the 2D kinematic forward model, we only considered the major structures interpreted on seismic lines due to the scale and the limitations of the available algorithms. The 2D kinematic forward model starts with the Crêt de la Neige thrusting (Fig. 9) and does not consider the structures south-east of this anticline. Therefore, In the Geneva Basin, the Triassic imbricates and the two south-verging faults, observed on seismic lines have been drawn manually in the final cross-section (Fig. 11). The south-verging faults could either be reverse faults or inherited normal faults passively displaced and deformed by the Jura thrusting. This question has not been addressed since it was beyond the scope of this paper.

6.2 Regional tectonics & kinematics

Based on the regional geological map and on our structural/kinematic understanding, we can propose a simplified map showing the main structural units and thus derive the regional kinematics which link the different faults, thrusts and fault-related folds of the study area

(See figure on next page.)

Fig. 12 a tectonic map with kinematic indicators showing the Jura nappes. The different coloured domains, NW of the Vuache Fault System in red, are the 7 tectonic nappes separated by the main thrusts rooting in the main décollement. Major displacement or transport directions (black arrows) are defined as being perpendicular to the fold and thrust orientations and depending on the sense of the thrust faults. The small white scheme on the map shows the regional kinematics of the Western Internal Jura. **b** The simplified final cross-section shows the Jura nappes in section view with their corresponding shortenings. Based on our 2D kinematic forward model, these values lead to a total shortening value of 23,6 km
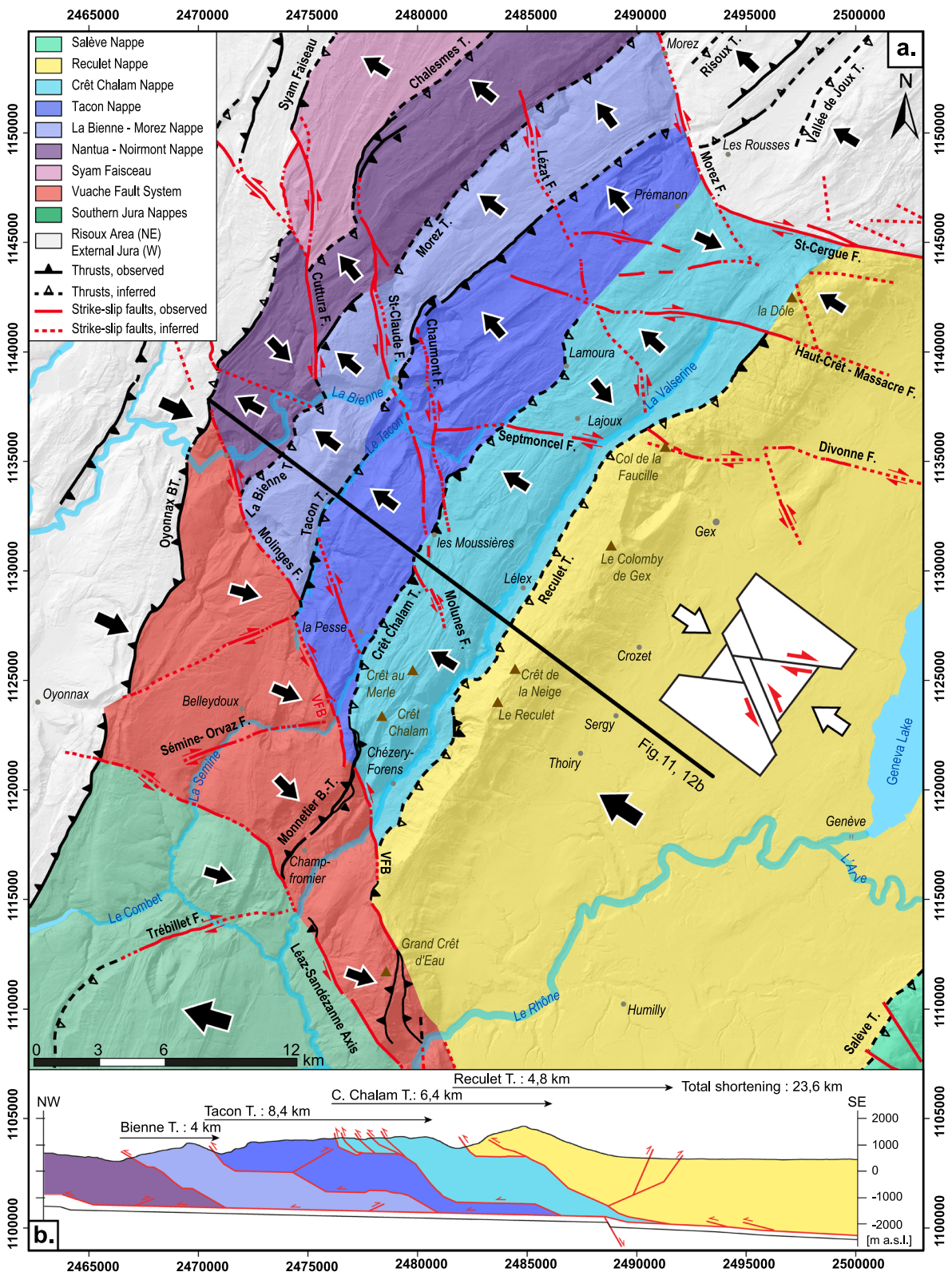
Fig. 12 (See legend on previous page.)

(Fig. 12). Major displacement or transport directions (black arrows on Fig. 12) are defined as being perpendicular to the fold and thrust orientations, and depend on the sense of movement on the thrusts (NW-verging thrusts or SE-verging thrusts). The major strike-slip faults act as a conjugated fault system and constrain a general shortening direction, oriented NW–SE with small local deviations. The shortening direction is thus parallel to the main transport direction.

The Vuache Fault System (VFS) and its prolongation to the north form the main strike-slip boundary to the west of our area of investigation (Fig. 12), while the St-Cergue – Les Morez Faults define the eastern boundary. The eastern branch of the Vuache Fault system (VFS) cuts the Reculet Thrust and forms an oblique ramp with the Crêt Chalam Thrust. Further north, the Molinges Fault which is considered as one of the en-échelon faults of the VFS, also forms an oblique ramp with the Bienne Thrust (Donzeau et al., 1998). The St-Cergue and Morez strike-slip Faults form the north-east boundary of the area. Unlike these major bounding faults, strike-slip faults such as the Haut-Crêt or St-Claude Faults have a more local influence and do not disturb the structural style and the general thrust orientations of the area.

The Western Internal Jura thrusts and anticlines between the VFS and the St-Cergue—Morez faults which are two major domain bounding fault systems can be subdivided into 7 distinct structural units (Fig. 12). According to the definitions of Lugeon (1902), Termier (1906), Tollmann (1973) (and references therein), we propose that these units are small-scale tectonic nappes, equivalent to the definition of "thrust sheets" after Suppe (1985). They are bound by a major basal thrust and laterally by steep faults (strike-slip faults), and show important displacement in excess of several kilometres. This concept of cover nappes is applied throughout our study area, and has been already suggested or hinted at in works by Rigassi (1962), Aubert (1971), Bitterli (1972), Wildi and Huggenberger (1993), Philippe et al., 1996, Aufranc et al. (2017) and Rime et al. (2019).

In the study area, the basal thrust of the 7 nappes root in the primary basal décollement; they are from south to north (Fig. 12): the Salève Nappe, the Reculet Nappe, the Crêt Chalam Nappe, the Tacon Nappe, the Bienne-Morez Nappe, the Nantua-Noirmont Nappe. The Syam Faisceau domain pertains already to the External Jura. They show a dominant top-to-the north transport and occasional backthrusting. We thus have a tectonic setting showing a thin-skinned style deformation, with stacking of nappes in the Mesozoic cover series.

6.3 Deep structures

The 2D kinematic forward model and the seismic interpretations validate a thin-skinned deformation style with multiple secondary décollements for the Western Internal Jura FTB (Figs. 7, 8, 9, 10). This solution is an alternative to the proposed thick evaporitic duplexes in the Keuper Group (see Signer & Gorin, 1995; Meyer, 2000; Morend, 2000; Charollais et al., 2007; Cardello et al., 2020), or basement highs resulting from the inversion of the Paleozoic basement structures such as inverted Permo-Carboniferous grabens (Guellec et al., 1990; Philippe et al., 1996).

Despite a seismic data gap under the Valserine Valley and the Crêt de la Neige summit, the change in inclination angle and elevation of the Near-Top Basement horizon between the Geneva Basin and the Jura FTB can be represented as a localised, discrete jump in the topography of the décollement. Similar basement steps have already been proposed in the vicinity of the study area (Guellec et al., 1990; Philippe et al., 1996) and across the Jura FTB (Chauve et al., 1988; Bergerat et al., 1990; Wildi & Huggenberger, 1993; Martin & Mercier, 1996; Philippe et al., 1996; Madritsch et al., 2008; Caër et al., 2018; Schori, 2021; Schori et al., 2021;). In some areas, the geometry and orientations of the Jura FTB thrusting and folding are significantly influenced by the topography of the basement and the strike of basement faults (Steinmann, 1902; Boigk & Schöneich, 1974; Allenbach & Wetzel, 2006; Laubscher, 2008; Meier, 2010; Caër et al., 2018; Schori, 2021; Schori et al., 2021). In the area of the VFS, basement steps have been recognised from seismic interpretations (Guellec et al., 1990). Schori et al. (2021) demonstrate with analogue models that these basement steps are inherited structures formed prior to the Jura FTB, and not a late basement inversion as suggested by Guellec et al. (1990) or Philippe (1995). Following the work of Schori (2021), the step situated under the south-east flank of the Crêt de la Neige Anticline is interpreted, to be a step due to a pre-existing, inherited normal fault in the basement, with an offset of 200 m (Fig. 8). This fault could correspond to the northern limit of a suspected Permo-Carboniferous graben interpreted by Gorin et al. (1993) and Clerc (2016), and reinterpreted on the depth-converted seismic lines GG87-02, 82GEX06 and SJ1U03 (Figs. 7b, 11).

The interpretation of tilted seismic reflectors at the southern end of our profile (Fig. 7b) has shown that thickening of the Triassic units in the Geneva Basin can be explained by the formation of imbricates and/or evaporite pillow structures. This thickening induces a gentle

antiformal structure in the Mesozoic cover, similarly to the low amplitude evaporite-cored anticlines interpreted under the Swiss Molasse Basin (Sommaruga et al., 2012). In the Jura FTB, large imbricates or pillows are observed on the 80-JU-01, 81-JU-06 and 82-JU-18 seismic lines (Fig. 7b). They significantly deform the overlying rock units and are likely responsible for local south verging thrusting along the main décollement as seen on seismic line 80-JU01 under the Bellecombe Anticline (Fig. 7b). In the footwall of the Bienne Thrust, the folding of the Mesozoic cover, interpreted on the 81-JU-06 seismic line, can either be induced by an evaporitic pillow or, a basement step (Figs. 7, 8). It must be emphasised that, alternatively, the latter structure could also be a seismic processing artefact. The zones showing thickening of the Keuper Group evaporite-rich layers are difficult to balance and therefore have been represented by small imbricate structures in the 2D kinematic forward model (Figs. 9, 10) and on the final cross-section (Fig. 11). In the 2D kinematic forward model, shortening of 600 m is accommodated by these Triassic evaporites, although a higher amount of shortening cannot be excluded, since more imbricates could be interpreted in the décollement zone (Fig. 7).

6.4 Shortening in the Western Internal Jura

The best-fit 2D kinematic forward model (Figs. 9, 10) yields a total amount of shortening of 23.6 km for the Western Internal Jura, from the Geneva Basin to the Bienne Valley. Previous kinematic models of the Western Jura Mountains, including the External Jura, using retrodeformation techniques, have been proposed by Philippe (1995), Affolter and Gratier (2004) and Schori (2021). Affolter and Gratier (2004) estimated a shortening amount of 26.3 km, Philippe (1995) and Schori (2021) calculated a shortening amount of 32 km for the entire Jura FTB (Internal and External). A cross-section along a similar section trace yield an amount of shortening of about 19 km by Philippe (1995) (section crossing the Mont Crêt d'Eau). Similarly to our model, Schori (2021) estimates a shortening of the study area of 20 km. Shortening amounts of 2.7 to 10 km are thus accommodated in the External Jura according to Philippe (1995), Affolter and Gratier (2004) and Schori (2021). The values of shortening of Philippe (1995), Affolter and Gratier (2004) and Schori (2021) are in the same order of magnitude as the shortening calculated in our study, but possibly underestimate shortening for the Internal Jura FTB with a minimum difference of 3 km. This difference is due to our multiple décollement approach. The flat of the Crêt Chalam Thrust under the Valserine Valley implies a larger displacement of the detached cover than previous solutions.

6.5 Sequence and dating of thrusting deformation

Overall, the Jura FTB can be described as a mechanical wedge propagating towards the northwestern foreland to override the Bresse Graben rift shoulder in its outer skirts. Internally, the mechanical wedge is achieving criticality by adjusting to the external processes such as erosion, changes in friction along the basal décollement, or in the décollement geometry (inclination, upward and downward steps) (Davis et al., 1983). This adjustment conditions the wedge-internal thrust sequence (Fig. 11). The 2D kinematic forward model developed in our study offers the possibility to assess this internal sequence, which has shown a possible general south-east to north-west forward stepping sequence, with minor back-stepping sequences (Figs. 9, 10, 11). The minor back-stepping sequences (Crêt Chalam imbricates and the Tacon south-verging Thrust) are interpreted to have occurred in order to re-equilibrate the critically tapered wedge by creating topography (Davis et al., 1983). Especially, the backstepping sequence of the Crêt de Chalam could be linked to the need to build excess topography in order to overcome the basement step below the present Molasse Basin—Internal Jura transition.

Absolute dating, chronostratigraphy, sedimentological analyses and seismic interpretations of angular onlapping of the Molasse units, found in the Geneva Basin and those on the Jura synclines, can be used to estimate the ages of the tectonic structures. Growth strata geometries and onlaps observed on seismic lines and in the field suggest that the main phase of the Jura deformation started during the Early Miocene (Rangheard et al., 1990; Deville et al., 1994; Beck et al., 1998). Based on chronostratigraphy, angular unconformities observed in the field, and on seismic lines of the dated syntectonic Molasse sequences, Kalifi et al. (2021) suggested that the activation of the Salève Thrust started at 18.05 ± 0.25 Ma. Further east, the activation of the Gros-Foug Thrust is dated at 17.35 ± 0.15 Ma. The thrusting in the more southerly Jura FTB has been set approximately at 16.2 Ma by Kalifi et al. (2021). These authors propose a forward stepping sequence of deformation for the Southern Jura FTB. Although, the link between the thrusts of our study area and the Southern Jura FTB remains difficult to ascertain because of the Vuache Fault System, this is in agreement with our 2D kinematic forward model.

Our results show that the Crêt de la Neige Anticline and the Reculet Thrust are the first structures to develop, prior to the Crêt Chalam Thrust and associated topography further to the north-west. This implies that the main topographic ridge initiated at the present transition between Molasse Basin and the Internal Jura FTB. The imbricate fault-bend folding developed beneath the

Crêt de la Neige explains the steepening of the ramp and the bedding of the resulting anticline. This implies that the Reculet Thrust developed first, before subsequently being tilted. This agrees with Donzeau et al. (1998) who suggest a kinematic evolution between the Vuache Fault, the Reculet Thrust and Crêt Chalam Thrust. The Crêt Chalam Thrust is connected in the present-day by oblique ramps to the VFB Fault, despite of the Reculet Thrust which stops abruptly against it (Figs. 2 and 3). Considering a forward stepping deformation (from SE to the NW), Donzeau et al. (1998) suggest that the Reculet Thrust formed first and was previously connected to the VFB Fault by an oblique ramp. Later, this connexion has been cut by the passive displacement of the Reculet nappe, induced by the Crêt Chalam thrusting (Fig. 9, steps 2 and 3) (Donzeau et al., 1998). If we consider a forward stepping sequence, the Salève Thrust, also situated in our study area, started before the Reculet Thrust. According to the dating of Kalifi et al., 2021, the Reculet Thrusting must, therefore, have been activated after 18.05 ± 0.25 Ma.

According to our 2D kinematic forward model, the Crêt Chalam thrust has been activated after the Reculet thrust. Charollais et al. (2006) dated the base of the Molasse deposits in the footwall of the Crêt Chalam Thrust (Fig. 2) to the Late Burdigalian age and suggest an Early Langhian age (16–14 Ma) for the summital unit. In this case, the Crêt Chalam thrusting over these deposits must have taken place after the Early Langhian age.

The steepness of the Crêt Chalam Thrust also implies the formation of an underlying imbricate fault-bend folding, in this case the Tacon Thrust. The implication is that the Tacon Thrust is the next major thrust developing in a forward stepping sequence.

Similarly, the steep dip data of both the south-east limb of the les Bouchoux Anticline (Fig. 2) and of the Tacon Thrust imply the emplacement of a younger ramp which in our case study is the Bienne Thrust. Additional ages dating directly the deformation and derived from calcite fibres U–Pb isotope, are available north-west of the Bienne Thrust. Smeraglia et al. (2021) dated the Molinges strike-slip Fault, near the Oyonnax Backthrust. Their results show that the fault was active at 10.5 ± 0.4, 9.1 ± 6.5, and 7.3 ± 1.9 Ma and reactivated in later stage at 4.8 ± 1.7 and at 0.72 ± 4.5 Ma. Since these calcite fibres are located northward of the Bienne Valley, the Bienne Thrust possibly has been active prior to 10.5 ± 0.4 Ma, if we consider that this strike-slip fault was coeval to the Jura thrusting and that we are still in a forward stepping sequence. From thrusting on top of Tertiary sediments in the Bresse Graben, we know that the deformation reached the External Jura at around 5 Ma (Michel et al., 1953), confirming the overall progression of deformation towards the foreland.

7 Conclusion

Recent works on the Geneva Basin area and in the adjacent Jura FTB made it possible to re-assess the structural geology of the Western Internal Jura FTB. New fieldwork, compilation and harmonisation of existing data, new maps, and seismic interpretation allowed us to obtain a new kinematically viable and balanced cross-section with deep structures validated by forward modelling.

Based on our new structural analysis and interpretation of subsurface structures and kinematic modelling, we draw the following conclusions:

(a) Major strike-slip faults act as a conjugated fault system. This system compartmentalises the whole area into distinct structural domains and constrains a general shortening direction, oriented NW–SE with small local deviations. The SSE-NNW oriented strike faults display a sinistral offset, while the WNW-ESE oriented strike-slip faults show a dextral offset. Discrete WNW-ESE major and dextral strike-slip faults are less developed in the area of investigation, but the dextral offset is accommodated by smaller and numerous strike-slip faults forming strike-slip corridors.

(b) The major thrusts and strike-slip faults constrain distinct tectonic domains, with a similar internal structural setting, that can be considered as small-scale tectonic nappes. Each of these nappes has a displacement in excess of several kilometres. We could identify 7 distinct nappes in the Internal Jura FTB, in addition to the structural domain of the Vuache Fault system and the Molasse basin domain.

(c) The Near-Top Basement horizon has been constrained with unprecedented accuracy by using seismic and well data. Beneath the Jura FTB domain, the Near-Top Basement horizon dips 1.3° to the south-east, whereas under the Geneva Basin, this dip is between 2.7° and 3.3° towards the south-east. This change in angle and also in altitude, occurs under the south-eastern flank of the Crêt de la Neige Anticline and has been interpreted to reflect and be associated with an inherited normal fault with a supposed offset of around 200 m in the basement.

(d) Our 2D kinematic forward model shows a thin-skinned deformation style with the main décollement situated at the base of the Keuper Group evaporites and three secondary décollements in the

marly layers of the Aalenian faciès de Transition units, the Oxfordian Couches d'Effingen-Geissberg members and the Berriasian Goldberg formation. Using such a multiple thrust horizon approach avoids having to introduce thick evaporitic duplexes in the Keuper Group, high basement horst or inverted Permo-Carboniferous graben structures to explain the high topographic position of the Western Jura folds. This hypothesis is supported by the interpreted depth-converted seismic lines.

(e) The 2D kinematic forward model yields a total shortening of 23.6 km for the Western Internal Jura, and shows an overall forward propagation with a locally oscillating thrust sequence. The first deformation is attributed to the Reculet Thrust and its secondary branch, possibly after 18 Ma. The second main deformation is attributed to the Crêt Chalam Thrust, with back-stepping imbrications as old as 14–16 Ma. The Tacon Thrust and the linked south-verging thrust, are defined to be the third main deformation event, occurred between 16 and 10 Ma. Finally, the last deformation of the Internal Western Jura FTB is the Bienne Thrust, which has possibly been active prior to 10 Ma.

(f) The oscillation of the Jura FTB thrust sequence is driven by the distance to criticality of the low angle alpine tapered wedge. The minor back-stepping sequences (Crêt Chalam imbrications and the Tacon south-verging thrust) are thus interpreted to occur in order to reequilibrate the critically tapered wedge.

Availability of data and materials
The datasets used and/or analysed during the current study are available from the corresponding author on reasonable request.

Declarations

Ethics approval and consent to participate
Not applicable.

Consent for publication
Not applicable.

Competing interests
The authors declare that they have no competing interests.

References

Affolter, T., & Gratier, J.-P. (2004). Map view retrodeformation of an arcuate fold-and-thrust belt: The Jura case. *Journal of Geophysical Research, 109*(B03404), 20. https://doi.org/10.1029/2002JB002270

Allenbach, R., Baumberger, R., Kurmann, E., Michael, C. S., & Reynolds, L. (2017). GeoMol: Geologisches 3D-Modell des Schweizer Molassebeckens: Schlussbericht. In *Berichte der Landesgeologie* (Vol. 10). Federal Office of Topography (Swisstopo).

Allenbach, R., & Wetzel, A. (2006). Spatial patterns of Mesozoic facies relationships and the age of the Rhenish Lineament: A compilation. *International Journal of Earth Sciences, 95*, 803–813. https://doi.org/10.1007/s00531-006-0071-0

Allmendinger, R. W. (1998). Inverse and forward numerical modeling of trishear fault-propagation folds. *Tectonics, 17*(4), 640–656. https://doi.org/10.1029/98TC01907

Antunes, V., Planès, T., Zahradník, J., Obermann, A., Alvizuri, C., Carrier, A., & Lupi, M. (2020). (2020) Seismotectonics and 1-D velocity model of the Greater Geneva Basin, France—Switzerland. *Geophysical Journal International, 221*(3), 2026–2047. https://doi.org/10.1093/gji/ggaa129

Aubert, D. (1971). Le Risoux, un charriage jurassien de grandes dimensions. *Eclogae Geologicae Helvetiae, 64*(1), 152–156. https://doi.org/10.5169/seals-163975

Aufranc, J., Jordan, P., Piquerez, A., Hofmann, B., Andres, B., & Burkhalter, R. (2017). Feuille 1125 Chasseral. Atlas Géol. Suisse 1:25'000, Notice Explicative 155, Federal Office of Topography (Swisstopo).

Beck, C., Deville, E., Blanc, E., Philippe, Y., & Tardy, M. (1998). Horizontal shortening control of Middle Miocene marine siliciclastic accumulation (Upper Marine Molasse) in the southern termination of the Savoy Molasse Basin (northwestern Alps/southern Jura). *Geological Society of London, Special Publications, 134*(1), 263–278. https://doi.org/10.1144/GSL.SP.1998.134.01.12

Becker, A. (2000). The Jura Mountains — an active foreland fold-and-thrust belt? *Tectonophysics, 321*(4), 381–406. https://doi.org/10.1016/S0040-1951(00)00089-5

Bellahsen, N., Mouthereau, F., Boutoux, A., Bellanger, M., Lacombe, O., Jolivet, L., & Rolland, Y. (2014). Collision kinematics in the western external Alps. *Tectonics, 33*(6), 1055–1088. https://doi.org/10.1002/2013TC003453

Bergerat, F., Mugnier, J.-L., Guellec, S., Truffert, C., Cazes, M., Damotte, B., & Roure, F. (1990). Extensional tectonics and subsidence of the Bresse basin: An interpretation from ECORS data. *Deep Structures of the Alps, 1*, 145–156.

Bitterli, P. (1972). Erdölgeologische Forschungen im Jura. *Bulletin der Vereinigung Schweiz. Petroleum-Geologen und -Ingenieure, 39*(95), 13–28.

Blondel, T., Charollais, J., Sambeth, U., & Pavoni, N. (1988). La faille du Vuache (Jura méridional): Un exemple de faille à caractère polyphasé. *Bulletin de la Société Vaudoise des Sciences Naturelles, 79*(2), 65–91.

Boigk, H., & Schöneich, H. (1974). Perm, Trias und älterer Jura im Bereich der südlichen Mittelmeer-Mjösen-Zone und des Rheingrabens. In J. H.

Illies & K. Fuchs (Eds.), *Approaches to Taphrogenesis: proceedings of an international Rift Symposium held in Karlsruhe, April 13–15, 1972 - Inter-Union Commission on Geodynamics, Scientific Report* (Vol. 8, pp. 60–71). Schweizerbart.

Borderie, S., Mosar, J., Hauvette, L., Marro, A., Sommaruga, A., & Meyer, M. (2022). Numerical modelling of current state of stress in the Geneva Basin and adjacent Jura fold-and-thrust belt (Switzerland and France) (No. EGU22-8449). Copernicus Meetings. 10.5194/egusphere-egu22-8449

Boutoux, A., Bellahsen, N., Nanni, U., Pik, R., Verlaguet, A., Rolland, Y., & Lacombe, O. (2016). Thermal and structural evolution of the external Western Alps: Insights from (U–Th–Sm)/He thermochronology and RSCM thermom-etry in the Aiguilles Rouges/Mont Blanc massifs. *Tectonophysics, 683*, 109–123. https://doi.org/10.1016/j.tecto.2016.06.010

Boyer, S., & Elliott, D. (1982). Thrust systems. *American Association of Petroleum Geologists Bulletin, 66*(9), 1196–1230.

Brandes, C., & Tanner, D. C. (2014). Fault-related folding: A review of kinematic models and their application. *Earth-Science Reviews, 138*, 352–370.

Brentini, M. (2018). *Impact d'une donnée géologique hétérogène dans la gestion des géo-ressources: analyse intégrée et valorisation de la stratigraphie à travers le bassin genevois (Suisse, France)* [Doctoral dissertation, University of Geneva].

BRGM (2020). *Infoterre*. Retrieved from http://infoterre.brgm.fr/viewer/MainTileForward.do. Accessed 20 Oct 2020.

Bucher, S., Schmid, S. M., Bousquet, R., & Fügenschuh, B. (2003). Late-stage deformation in a collisional orogen (Western Alps): Nappe refolding, back-thrusting or normal faulting? *Terra Nova, 15*(2), 109–117. https://doi.org/10.1046/j.1365-3121.2003.00470.x

Burkhard, M. (1990). Aspects of the large-scale Miocene deformation in the most external part of the Swiss Alps (Subalpine Molasse to Jura fold belt). *Eclogae Geologicae Helvetiae, 83*(3), 559–583. https://doi.org/10.5169/seals-166602

Burkhard, M., & Sommaruga, A. (1998). Evolution of the western Swiss Molasse basin: Structural relations with the Alps and the Jura belt. *Geological Society, London, Special Publications, 134*, 279–298. https://doi.org/10.1144/GSL.SP.1998.134.01.13

Butler, R. W., Bond, C. E., Cooper, M. A., & Watkins, H. (2018). Interpreting structural geometry in fold-thrust belts: Why style matters. *Journal of Structural Geology, 114*, 251–273. https://doi.org/10.1016/j.jsg.2018.06.019

Buxtorf, A. (1907). Zur Tektonik des Kettenjura. *Bericht der Versammlung des Oberrheinischen Geologischen Vereins, 40*, 29–38.

Caër, T., Souloumiac, P., Maillot, B., Leturmy, P., & Nussbaum, C. (2018). Propagation of a fold-and-thrust belt over basement graben. *Journal of Structural Geology, 40*, 121–131.

Cardello, G. L., Carminati, E., Doglioni, C., & Mercuri, M. (2020). *Fault and fold control in a karst geothermal system: internal Jura mountains and Geneva Basin (France and Switzerland)*. (Report No. 1). Sapienza University of Rome.

Carrier, A., Nawratil de Bono, C., & Lupi, M. (2020). Affordable gravity prospec-tion calibrated on improved time to depth conversion of old seismic profiles for exploration of geothermal resources. *Geothermics, 86*, 101800.

Charollais, J.-J., Weidmann, M., Berger, J.-P., Engesser, B., Hotellier, J.-F., Gorin, G. E., Reichenbacher, B., & Schäfer, P. (2007). La Molasse du bassin franco-genevois et son substratum. *Archives Des Sciences, 60*, 59–174.

Charollais, J.-J., Wernli, R., Du Chene, R. J., Von Salis, K., & Steiner, F. (2006). La Molasse marine supérieure de la Combe d'Evuaz et de la Pesse. *Archives des Sciences, 59*, 21–46.

Chauve, P., Martin, J., Petitjean, E., & Sequeiros, F. (1988). Le chevauchement du Jura sur la Bresse. Données nouvelles et réinterprétation des sondages. *Bulletin de la Société Géologique de France*. https://doi.org/10.2113/gssgfbull.IV.5.861

Chauve, P., & Perriaux, J. (1974). Le jura. In Debelmas, J. (Ed.), *Géologie de la France: les chaînes plissées du cycle alpin et leur avant-pays* (Vol. 2, pp. 443–464). Doin.

Clerc, N. (2016). *GeoMol-CH project: Interpretation and modeling report of the Geneva area*. (Report No. 201600001), Geo-Energy Group, University of Geneva.

Clerc, N. (2022). *A revised structural framework across the Geneva Basin and neighbouring France as revealed from 2D seismic data* (Doctoral disserta-tion, University of Geneva).

Clerc, N., & Moscariello, A. (2020). A revised structural framework for the Geneva Basin and the neighboring France region as revealed from 2D seismic data: Implications for geothermal exploration. *Swiss Bulletin for Applied Geology, 25*, 109–131.

Davis, D., & Engelder, T. (1985). The role of salt in fold-and-thrust belts. *Tectonophysics, 119*(1–4), 67–88. https://doi.org/10.1016/0040-1951(85)90033-2

Davis, D., Suppe, J., & Dahlen, F. A. (1983). Mechanics of fold-and-thrust belts and accretionary wedges. *Journal of Geophysical Research: Solid Earth, 88*(B2), 1153–1172. https://doi.org/10.1029/JB088iB02p01153

Deville, E. (1990). Chronostratigraphie et lithostratigraphie synthétique du Jurassique supérieur et du Crétacé inférieur de la partie méridionale du Grand Salève (Haute-Savoie, France). *Archives Des Sciences, Genève, 43*, 215–235.

Deville, E., Blanc, E., Tardy, M., Beck, C., Cousin, M., Ménard, G. (1994). Thrust Propagation and Syntectonic Sedimentation in the Savoy Tertiary Molasse Basin (Alpine Foreland). In: Mascle, A. (eds) *Hydrocarbon and Petroleum Geology of France. Special Publication of the European Associa-tion of Petroleum Geoscientists* (vol 4, pp. 269–280). Springer, Berlin, Heidelberg. https://doi.org/10.1007/978-3-642-78849-9_19

Deville, E., & Sassi, W. (2006). Contrasting thermal evolution of thrust systems: An analytical and modeling approach in the front of the western Alps. *American Association of Petroleum Geologists Bulletin, 90*(6), 887–907. https://doi.org/10.1306/01090605046

Do Couto, D., Garel, S., Moscariello, A., Daher, S. B., Littke, R., & Weniger, P. (2021). Origins of hydrocarbons in the Geneva Basin: Insights from oil, gas and source rock organic geochemistry. *Swiss Journal of Geosciences, 114*, 1–28.

Donzeau, M., Wernli, M., Charollais, J., & Monjuvent, G. (1997). *Carte géol. France (1/50 000), feuille Saint-Julien-en-Genevois (653)* (p. 144). BRGM France.

Donzeau, M., Wernli, R., & Charollais, J. (1998). Interprétation nouvelle de la géométrie de l'accident du Vuache dans le Jura méridional: Le relais de failles transpressif sénestre Léaz-Champfromier (Ain). *Géologie De La France, 2*, 25–45.

Egal, E. (2007). *Carte géologique harmonisée du département de l'Ain.* (Rapport final No. 55512-FR). BRGM, France.

Egan, S. S., Buddin, T. S., Kane, S., & Williams, G. D. (1997). Three-dimensional modelling and visualisation in structural geology: new techniques for the restoration and balancing of volumes. In *Proceedings of the 1996 Geoscience Information Group Conference on Geological Visualisation, Electronic Geology Special* (Vol. 1, pp. 67–82).

Endignoux, L., & Mugnier, J.-L. (1990). The use of a forward kinematic model in the construction of balanced cross sections. *Tectonics, 9*(5), 1249–1262. https://doi.org/10.1029/TC009i005p01249

Erslev, E. A. (1991). Trishear fault-propagation folding. *Geology, 19*(6), 617–620.

Giamboni, M., Ustaszewski, K., Schmid, S. M., Schumacher, M. E., & Wetzel, A. (2004). Plio-Pleistocene transpressional reactivation of Paleozoic and Paleogene structures in the Rhine-Bresse transform zone (northern Switzerland and eastern France). *International Journal of Earth Sciences, 93*, 207–223. https://doi.org/10.1007/s00531-003-0375-2

Gorin, G., Signer, C., & Amberger, G. (1993). Structural configuration of the western Swiss Molasse Basin as defined by reflection seismic data. *Eclogae Geologicae Helvetiae, 86*(3), 693–716.

Guellec, S., Mugnier, J.-L., Tardy, M., & Roure, F. (1990). Neogene evolution of the western Alpine foreland in the light of ECORS data and balanced cross sections. In F. Roure, P. Heitzmann, & R. Polino (Eds.), *Deep structures of the Alps* (1st ed.), Mémoires de la Société géologique Suisse, 165–185.

Guglielmetti, L., Heidinger, M., Eichinger, F., & Moscariello, A. (2022). Hydro-chemical characterization of groundwaters'fluid flow through the upper mesozoic carbonate geothermal reservoirs in the Geneva Basin: An evolution more than 15,000 years long. *Energies, 15*(10), 3497. https://doi.org/10.3390/en15103497

Guillaume, A., Llac, F., & Meurisse, M. (1972). *Notice explicative de la carte géologique de la France (1/50'000), feuille Saint-Claude (149)* (p.16). BRGM France.

Hardy, S., & Allmendinger, R. W. (2011). Trishear: A Review of Kinematics, Mechanics, and Applications. In K. McClay, Shaw J, & J. Suppe (Eds.), *Thrust fault-related folding* (pp. 95–119). AAPG Memoir (94). https://doi.org/10.1306/13251334m943429

Hauvette, L., Marro, A., Borderie, S., Sommaruga, A., & Mosar, J. (2021). *3D Seismic Model from Salève to Jura*. University of Fribourg.

Homberg, C., Bergerat, F., Philippe, Y., Lacombe, O., & Angelier, J. (2002). Structural inheritance and Cenozoic stress fields in the Jura fold-and-thrust belt (France). *Tectonophysics, 357*(1–4), 137–158.

Hydro-Geo Environnement. (2018). *GEo-01—Litholog de forage,* (No Mandat. 1281), Genève.

Hydro-Geo Environnement. (2020). *GEo-02—Litholog de forage,* (No Mandat. 1451), Genève.

IGN-F. (2018). *MNT RGE ALTI 5m, Digital Elevation Models*. Institut national de l'information géographique et forestière (IGN-F). Retrieved from http://www.ign.fr. Accessed 23 Apr 2020.

Jordan, P. (1992). Evidence for large-scale decoupling in the Triassic evaporites of northern Switzerland: An overview. *Eclogae Geologicae Helvetiae, 85*(3), 677–693. https://doi.org/10.5169/seals-167025

Jordan, P. (2016). Reorganisation of the Triassic stratigraphic nomenclature of northern Switzerland: Overview and the new Dinkelberg, Kaiseraugst and Zeglingen formations. *Swiss Journal of Geosciences, 109*, 241–255. https://doi.org/10.1007/s00015-016-0209-4

Kalifi, A., Leloup, P. H., Sorrel, P., Galy, A., Demory, F., Spina, V., Huet, B., Quillévéré, F., Ricciardi, F., Michoux, D., Lecacheur, K., Grime, R., Pittet, B., & Rubino, J.-L. (2021). Chronology of thrust propagation from an updated tectono-sedimentary framework of the Miocene molasse (western Alps). *Solid Earth, 12*, 2735–2771. https://doi.org/10.5194/se-12-2735-2021

Lacombe, O., & Mouthereau, F. (2002). Basement-involved shortening and deep detachment tectonics in forelands of orogens: Insights from recent collision belts (Taiwan, Western Alps, Pyrenees). *Tectonics, 21*, 1–22. https://doi.org/10.1029/2001TC901018

Lanza, F., Diehl, T., Deichmann, N., Kraft, T., Nussbaum, C., Schefer, S., & Wiemer, S. (2022). The Saint-Ursanne earthquakes of 2000 revisited: evidence for active shallow thrust-faulting in the Jura fold-and-thrust belt. *Swiss Journal of Geosciences*. https://doi.org/10.1186/s00015-021-00400-x

Laubscher, H.-P. (1961). Die Fernschubhypothese der Jurafaltung. *Eclogae Geologicae Helvetiae, 54*(1), 222–282. https://doi.org/10.5169/seals-162820

Laubscher, H.-P. (1965). Ein kinematisches Modell der Jurafaltung. *Eclogae Geologicae Helvetiae, 58*(1), 232–318. https://doi.org/10.5169/seals-163266

Laubscher, H.-P. (2008). The Grenchenberg conundrum in the Swiss Jura: A case for the centenary of the thin-skin décollement nappe model (Buxtorf 1907). *Swiss Journal of Geosciences, 101*, 41–60. https://doi.org/10.1007/s00015-008-1248-2

Leloup, P. H., Arnaud, N., Sobel, E. R., & Lacassin, R. (2005). Alpine thermal and structural evolution of the highest external crystalline massif: The Mont Blanc. *Tectonics, 24*(4), 1–26. https://doi.org/10.1029/2004TC001676

Looser, N., Madritsch, H., Guillong, M., Laurent, O., Wohlwend, S., & Bernasconi, S. M. (2021). Absolute age and temperature constraints on deformation along the basal décollement of the Jura fold-and-thrust belt from carbonate U-Pb dating and clumped isotopes. *Tectonics*. https://doi.org/10.1029/2020TC006439

Lugeon, M. (1902). Les grandes nappes de recouvrement des Alpes du Chablais et de la Suisse. *Bull Soc Géol France, 4*, 723.

Madritsch, H., Schmid, S. M., & Fabbri, O. (2008). Interactions between thin- and thick-skinned tectonics at the northwestern front of the Jura fold-and-thrust belt (eastern France). *Tectonics*. https://doi.org/10.1029/2008TC002282

Malvésy, T., Tripet, J.-P., & Schaer, J.-P. (2021). *Histoire de la connaissance géologique du Jura franco-suisse*. Editions Alphil—Presses Universitaires Suisses.

Malz, A., Madritsch, H., Meier, B., & Kley, J. (2016). An unusual triangle zone in the external northern Alpine foreland (Switzerland): Structural inheritance, kinematics and implications for the development of the adjacent Jura fold-and-thrust belt. *Tectonophysics, 670*, 127–143. https://doi.org/10.1016/j.tecto.2015.12.025

Marti, J. (1969). *Rapport de fin de sondage d'Humilly 2*. (No de rapport. N773, 16–1185). Société Nationale des Pétroles d'Aquitaine (SNPA), direction exploration et production, division Europe.

Martin, J., & Mercier, É. (1996). Héritage distensif et structuration chevauchante dans une chaîne de couverture: Apport de l'équilibrage par modélisation géométrique dans le Jura nord-occidental. *Bulletin de la Société Géologique de France, 167*(1), 101–110.

Medwedeff, D. A., & Suppe, J. (1997). Multibend fault-bend folding. *Journal of Structural Geology, 19*(3–4), 279–292. https://doi.org/10.1016/S0191-8141(97)83026-X

Meier, B. P. (2010). Ergänzende Interpretation reflexionsseismischer Linien zwischen dem östlichen und westlichen Molassebecken. In NAGRA (Ed.), *NAGRA Arbeitsbericht 10–40*.

Meyer, M. (2000). *Le complexe récifal kimméridgien—tithonien du Jura méridional interne (France), évolution multifactorielle, stratigraphique et tectonique* (thèse de doctorat, Université de Genève).

Michel, P., Appert, G., Lavigne, J., Lefavrais, A., Bonte, A., Liénhardt, G., & Ricour, J. (1953). Le contact Jura-Bresse dans la région de Lons-le-Saunier. *Bulletin de la Société Géologique de France*. https://doi.org/10.2113/gssgfbull.s6-iii.7-8.593

Morend, D. (2000). *High-resolution seismic facies of alluvial depositional systems in the Lower Freshwater Molasse (Oligocene-early Miocene, western Swiss Molasse Basin)* [Doctoral dissertation, University of Geneva].

Mosar, J. (1999). Present-day and future tectonic underplating in the western Swiss Alps: Reconciliation of basement/wrench-faulting and décollement folding of the Jura and Molasse basin in the Alpine foreland. *Earth and Planetary Science Letters, 173*(3), 143–155. https://doi.org/10.1016/S0012-821X(99)00238-1

Moscariello, A., Guglielmetti, L., Omodeo-Salé, S., de Haller, A., Eruteya, O. E., Ying Lo, H., Clerc, N., Makloufhi, Y., do Couto, D., Ferreira de Oliveira, G., Perozzi, L., DeOliveira, F., Hollmuller, P., Quiquerez, L., Nawratil De Bono, C., Martin, F., & Meyer, M. (2020). Heat production and storage in Western Switzerland: advances and challenges of intense multidisplinary geothermal exploration activities, an 8 years progress report. In *Proceedings World Geothermal Congress* (p.12).

Mudry, J., & Rosenthal, P. (1977). *La Haute-Chaîne du Jura entre Morez, Saint-Claude et la Pesse. Étude géologique et hydrologique* (thèse de doctorat, Université de Franche-Comté).

Nagel, J. L. (2007). *Carte géologique harmonisée du département du Jura.* (Rapport final No. 55733-FR). BRGM, France.

Noack, T. (1995). Thrust development in the eastern Jura Mountains related to pre-existing extensional structures. *Tectonophysics, 252*(1–4), 419–431. https://doi.org/10.1016/0040-1951(95)00089-5

Nussbaum, C., Kloppenburg, A., Caër, T., & Bossart, P. (2017). Tectonic evolution around the Mont Terri rock laboratory, northwestern Swiss Jura: Constraints from kinematic forward modelling. *Swiss Journal of Geosciences, 110*, 39–66. https://doi.org/10.1007/s00015-016-0248-x

Pfiffner, O. A. (2014). *Geology of the Alps* (2nd ed.). John Wiley & Sons Blackwell.

Pfiffner, O. A. (2017). Thick-skinned and thin-skinned tectonics: A global perspective. *Geosciences (switzerland), 7*(3), 71. https://doi.org/10.3390/geosciences7030071

Philippe, Y. (1995). *Rampes latérales et zones de transfert dans les chaînes plissées: géométrie, conditions de formation et pièges structuraux associés* (thèse de Doctorat, Université de Savoie).

Philippe, Y., Colletta, B., Deville, E., & Mascle, A. (1996). The Jura fold-and-thrust belt: A kinematic model based on map-balancing. *Mémoires du Muséum National d'histoire Naturelle, 1993*(170), 235–261.

Poblet, J., & Lisle, R. J. (2011). Kinematic evolution and structural styles of fold-and-thrust belts. *Geological Society, London, Special Publications, 349*(1), 1–24. https://doi.org/10.1144/SP349.1

Rabin, M., Sue, C., Walpersdorf, A., Sakic, P., Albaric, J., & Fores, B. (2018). Present-day deformations of the Jura arc inferred by GPS surveying and earthquake focal mechanisms. *Tectonics, 37*(10), 3782–3804. https://doi.org/10.1029/2018TC005047

Rangheard, Y., Demarcq, G., Muller, C., Poignant, A., & Pharisat, A. (1990). Données nouvelles sur le Burdigalien du Jura interne; Paléobiologie, biostratigraphie et évolution structurale. *Bulletin de la Société Géologique de France, V, I*(3), 479–486. https://doi.org/10.2113/gssgfbull.VI.3.479

Ricchi, E., Bergemann, C. A., Gnos, E., Berger, A., Rubatto, D., & Whitehouse, M. J. (2019). Constraining deformation phases in the Aar Massif and the Gotthard Nappe (Switzerland) using Th-Pb crystallization ages of fissure monazite-(Ce). *Lithos, 342–343*, 223–238. https://doi.org/10.1016/j.lithos.2019.04.014

Rigassi, D. A. (1962). A propos de la tectonique du Risoux (Jura vaudois et franc-comtois). *Bulletin der Vereinigung Schweiz Petroleum-Geologen und -Ingenieure, 29*(76), 39–50.

Rime, V., Sommaruga, A., Schori, M., & Mosar, J. (2019). Tectonics of the Neuchâtel Jura Mountains: Insights from mapping and forward modelling. *Swiss Journal of Geosciences, 112*, 563–578. https://doi.org/10.1007/s00015-019-00349-y

Rusillon, E. (2017). *Characterisation and rock typing of deep geothermal reservoirs in the Greater Geneva Basin (Switzerland & France)* (Doctoral dissertation, University of Geneva).

Schori, M., Zwaan, F., Schreurs, G., & Mosar, J. (2021). Pre-existing basement faults controlling deformation in the Jura mountains fold-and-thrust belt: insights from analogue models. *Tectonophysics, 814*, 228980. https://doi.org/10.1016/j.tecto.2021.228980

Schori, M. (2021). *The development of the Jura fold-and-thrust belt: Pre-existing basement structures and the formation of ramps* (Doctoral dissertation, University of Fribourg). GeoFocus, 50, 200. https://doi.org/10.51363/unifr.sth.2022.001

Schori, M., Mosar, J., & Schreurs, G. (2015). Multiple décollements during thin-skinned deformation of the Swiss Central Jura: A kinematic model across the Chasseral. *Swiss Journal of Geosciences, 108*, 327–343. https://doi.org/10.1007/s00015-015-0196-x

Seward, D., & Mancktelow, N. S. (1994). Neogene kinematics of the central and western Alps: Evidence from fission-track dating. *Geology, 22*(9), 803–806. https://doi.org/10.1130/0091-7613(1994)022%3c0803:NKOTCA%3e2.3.CO;2

Signer, C., & Gorin, G. E. (1995). New geological observations between the Jura and the Alps in the Geneva area, as derived from reflection seismic data. *Eclogae Geologicae Helvetiae, 88*(2), 235–265. https://doi.org/10.5169/SEALS-167674

SITG (Système d'information du territoire à Genève) (2018). *MNA relief ombre surface 2017*. Retrieved from https://ge.ch/sitg/sitg_catalog/. Accessed 23 Apr 2019

Smeraglia, L., Looser, N., Fabbri, O., Choulet, F., Guillong, M., & Bernasconi, S. (2021). U-Pb dating of middle Eocene-middle Pleistocene multiple tectonic pulses in the Alpine foreland. In *Solid Earth Discussions* (pp. 1–14). 10.5194/se-12-2539-2021

Sommaruga, A. (1999). Décollement tectonics in the Jura foreland fold-and-thrust belt. *Marine and Petroleum Geology, 16*(2), 111–134. https://doi.org/10.1016/S0264-8172(98)00068-3

Sommaruga, A. (1997). Geology of the Central Jura and the Molasse Basin: New insight into an evaporite-based foreland fold and thrust belt. *Mémoire de la Société Neuchâteloise des Sciences Naturelles, 12*, 1–176.

Sommaruga, A., Eichenberger, U., & Marillier, F. (2012). Seismic Atlas of the Swiss Molasse Basin. In E. Kissling (Ed.), *Matériaux pour la Géologie de la Suisse—Géophysique* (Vol. 44, p. 90). Federal Office of Topography (swisstopo).

Sommaruga, A., Mosar, J., Schori, M., & Gruber, M. (2017). The Role of the Triassic Evaporites Underneath the North Alpine Foreland. In J. I. Soto, J. Flinch, & G. Tari (Eds.), *Permo-Triassic Salt Provinces of Europe, North Africa and the Atlantic Margins* (pp. 447–466). Elsevier. https://doi.org/10.1016/b978-0-12-809417-4.00021-5

Steinmann, G. (1902). Zur Tektonik des nordschweizerischen Kettenjura. *Centralblatt Für Mineralogie, Geologie Und Paläontologie Stuttgart*, (pp. 488–492).

Strasky, S., Morard, A., & Möri, A. (2016). Harmonising the lithostratigraphic nomenclature: Towards a uniform geological dataset of Switzerland. *Swiss Journal of Geosciences, 109*, 123–136. https://doi.org/10.1007/s00015-016-0221-8

Suppe, J. (1983). Geometry and kinematics of fault-bend folding. *American Journal of Science, 283*, 684–721.

Suppe, J. (1985). *Principles of structural geology*. Prentice Hall.

Swisstopo (2011). *Digital elevation model swissALTI3D*. Federal Office of Topography (Swisstopo). Retrieved from http://www.swisstopo.ch. Accessed 27 Nov 2019.

Termier, P. (1906). La synthèse géologique des Alpes. In : À la Gloire de la Terre, Desclée de Brouwer, Paris, (3e édition) [1922]. Conférence du 26 janvier 1906 devant les professeurs et les élève des Écoles spéciales et de l'Université de Liège (p. 43–82)

Tollmann, A. (1973). *Grundprinzipien der alpinen Deckentektonik: eine Systemanalyse am Beispiel der nördlichen Kalkalpen* (Vol. 1). Deuticke

Trümpy, R. (1980). An Outline of the Geology of Switzerland. In R. Trümpy (Ed.) *Geology of Switzerland, a guidebook: 10th International Geological Congress* (p. 334). Wepf & Co. Publishers.

Ustaszewski, K., & Schmid, S. M. (2007). Latest Pliocene to recent thick-skinned tectonics at the Upper Rhine Graben - Jura Mountains junction. *Swiss Journal of Geosciences, 100*, 293–312. https://doi.org/10.1007/s00015-007-1226-0

Ustaszewski, K., Schumacher, M. E., Schmid, S. M., & Nieuwland, D. (2005). Fault reactivation in brittle-viscous wrench systems—Dynamically scaled analogue models and application to the Rhine-Bresse Transfer Zone. *Quaternary Science Reviews, 24*, 363–380. https://doi.org/10.1016/j.quascirev.2004.03.015

van Mount, S., Suppe, J., & Hook, S. C. (1990). A forward modelling strategy for balancing cross sections. *American Association of Petroleum Geologists Bulletin, 74*(5), 521–531.

von Hagke, C., Cederbom, C. E., Oncken, O., Stöckli, D. F., Rahn, M. K., & Schlunegger, F. (2012). Linking the northern Alps with their foreland: The latest exhumation history resolved by low-temperature thermochronology. *Tectonics*. https://doi.org/10.1029/2011TC003078

Wildi, W., Blondel, T., Charollais, J., Jaquet, J.-M., & Wernli, R. (1991). Tectonique en rampe latérale à la terminaison occidentale de la Haute-Chaîne du Jura. *Eclogae Geologicae Helvetiae, 84*(1), 265–277.

Wildi, W., & Huggenberger, P. (1993). Reconstitution de la plate-forme européenne anté-orogénique de la Bresse aux Chaînes Subalpines; éléments de cinématique alpine (France et Suisse occidentale). *Eclogae Geologicae Helvetiae, 86*(1), 47–64.

Ziesch, J., Tanner, D. C., & Krawczyk, C. M. (2014). Strain associated with the fault-parallel flow algorithm during kinematic fault displacement. *Mathematical Geosciences, 46*, 59–73. https://doi.org/10.1007/s11004-013-9464-3

Zoetemeijer, R., & Sassi, W. (1992). 2-D reconstruction of thrust evolution using the fault-bend fold method. In K. R. McClay (Ed.), *Thrust Tectonics* (pp. 133–140). Dordrecht: Springer. 10.1007/978-94-011-3066-0_11.

Publisher's Note